molecular microbiology

Insulation and wiring specificity of BceR-like response regulators and their target promoters in *Bacillus subtilis*

Journal:	*Molecular Microbiology*
Manuscript ID	MMI-2016-16214.R1
Manuscript Type:	Research Article
Date Submitted by the Author:	04-Dec-2016
Complete List of Authors:	Fang, Chong; Ludwig-Maximilians-Universitaet, Biologie/Mikrobiologie Nagy-Staron, Anna; Institute of Science and Technology Austria, n.a. Grafe, Martin; Helmholtz Zentrum Munchen Deutsches Forschungszentrum fur Umwelt und Gesundheit, Research Unit Environmental Genomics Heermann, Ralf; LMU München, Mikrobiologie Jung, Kirsten; Ludwig-Maximilians-Universitaet, Biologie/Mikrobiologie Gebhard, Susanne; University of Bath, Biology and Biochemistry Mascher, Thorsten; Technische Universität Dresden, Institute of Microbiology
Key Words:	two-component system, promoter recognition, antimicrobial peptide resistance, response regulator, DNA-binding site

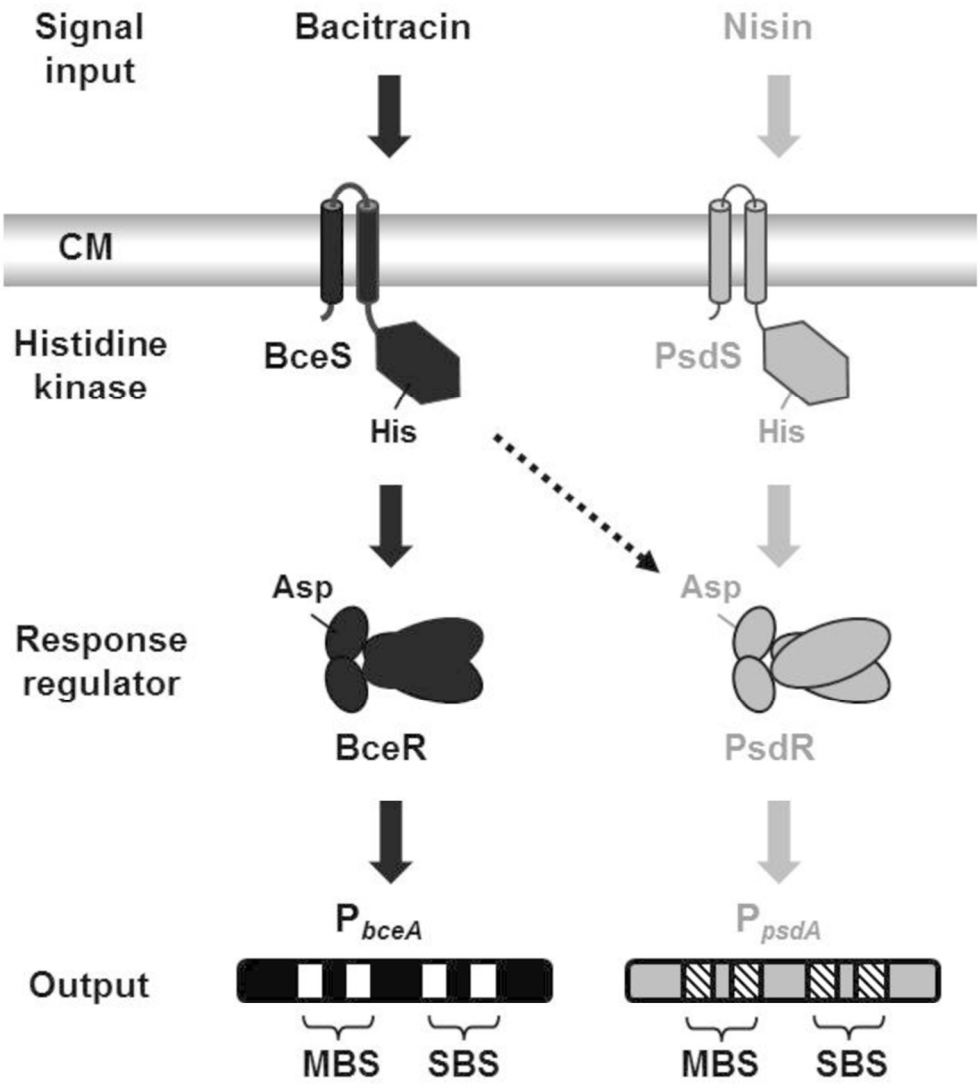

Model of signal transduction pathways of two Bce-like systems after induction with corresponding AMPs in Bacillus subtilis. The TCSs Bce and Psd and their inducing antibiotics as signal inputs are highlighted black and grey, respectively. For reasons of simplicity, the ABC transporters of both systems are not shown. Solid arrows indicate the signal transduction pathway within one system, while cross-regulation between BceS and PsdR is highlighted by the dotted arrow. On each promoter, MBS representing for the main binding site and SBS representing for the secondary binding of Bce-like RRs are filled with white on bceA promoter and slashes on psdA promoter. CM, cell membrane.

84x94mm (300 x 300 DPI)

Insulation and wiring specificity of BceR-like response regulators and their target promoters in *Bacillus subtilis*

*Chong Fang[1§], Anna Nagy-Staroń[1,3§], Martin Grafe[1], Ralf Heermann[1,2], Kirsten Jung[1,2], Susanne Gebhard[1,4], and Thorsten Mascher[1,5]**

Abbreviated summary

An efficient insulation is essential to ensure wiring specificity of highly similar signal transducing systems. Here, we describe the regulatory features necessary to allow discrimination of two target promoters by their corresponding paralogous response regulators, involved in mediating resistance against antimicrobial peptides in *Bacillus subtilis*. We demonstrate that regulator competition in combination with hierarchical cooperative binding ensures specificity despite only slight differences in binding affinities.

Insulation and wiring specificity of BceR-like response regulators and their target promoters in *Bacillus subtilis*

Chong Fang[1§], *Anna Nagy-Staroń*[1,3§], *Martin Grafe*[1], *Ralf Heermann*[1,2], *Kirsten Jung*[1,2], *Susanne Gebhard*[1,4], *and Thorsten Mascher*[1,5]*

[1]Department Biology I, Ludwig-Maximilians-Universität München, Großhaderner Str. 2-4, 82152 Martinsried, Germany

[2]Munich Center for Integrated Protein Science (CiPSM) at the Department Biology I, Ludwig-Maximilians-Universität München, Großhaderner Str. 2-4, 82152 Martinsried, Germany

[3]Institute of Science and Technology (IST) Austria, Am Campus 1, A-3400 Klosterneuburg, Austria

[4]Milner Centre for Evolution, Department of Biology and Biochemistry, University of Bath, Claverton Down, Bath BA2 7AY, United Kingdom

[5]Institute of Microbiology, Technische Universität (TU) Dresden, 01062 Dresden, Germany

Running title: Wiring specificity of Bce-like systems

Key words: two-component system, promoter recognition, antimicrobial peptide resistance, bacitracin, DNA-binding site

§ These two authors contributed equally to this work.

*To whom correspondence should be addressed. E-mail: thorsten.mascher@tu-dresden.de; Phone: +49 351 463-40420

Summary

BceRS and PsdRS are paralogous two-component systems in *Bacillus subtilis* controlling the response to antimicrobial peptides. In the presence of extracellular bacitracin and nisin, respectively, the two response regulators (RRs) bind their target promoters, P_{bceA} or P_{psdA}, resulting in a strong up-regulation of target gene expression and ultimately antibiotic resistance. Despite high sequence similarity between the RRs BceR and PsdR and their known binding sites, no cross-regulation has been observed between them. We therefore investigated the specificity determinants of P_{bceA} and P_{psdA} that ensure the insulation of these two paralogous pathways at the RR-promoter interface. *In vivo* and *in vitro* analyses demonstrate that the regulatory regions within these two promoters contain three important elements: in addition to the known (main) binding site, we identified a linker region and a secondary binding site that are crucial for functionality. Initial binding to the high affinity, low specificity main binding site is a prerequisite for the subsequent highly specific binding of a second RR dimer to the low affinity secondary binding site. In addition to this hierarchical cooperative binding, discrimination requires a competition of the two RRs for their respective binding site mediated by only slight differences in binding affinities.

Introduction

Antimicrobial peptides (AMPs) are predominantly produced by Gram-positive microbes to suppress the growth of competitors in their natural habitats (Berdy, 2005). The main target of AMPs is the bacterial cell envelope, especially different intermediates of the lipid II cycle. By binding to their target molecules, AMPs inhibit cell wall biosynthesis and cause cell death (Silver, 2003, Breukink & de Kruijff, 2006, Jordan *et al.*, 2008).

In Firmicutes bacteria, sensing of and resistance against AMPs is usually mediated by highly conserved Bce-like detoxification modules containing an ATP-binding-cassette (ABC) transporter and a two-component system (TCS) (Dintner *et al.*, 2011). The genome of *Bacillus subtilis* encodes three such systems: BceRS-BceAB, PsdRS-PsdAB and the poorly understood YxdJK-YxdLM-YxeA system (Joseph *et al.*, 2002, Gebhard & Mascher, 2011). The BceRS-BceAB paradigm responds to AMPs such as bacitracin, actagardine and mersacidin (Staroń *et al.*, 2011, Dintner *et al.*, 2014, Fritz *et al.*, 2015). It consists of two separate operons: the *bceRS* operon encodes the TCS comprised of a membrane anchored histidine kinase (HK), BceS, and a cytoplasmic response regulator (RR), BceR, under the control of a constitutive promoter. The *bceAB* operon encodes the ABC transporter under the control of an inducible BceR-dependent promoter, P_{bceA}. In the absence of AMPs, both operons are expressed at a very low level. In the presence of AMPs such as bacitracin, the ABC transporter BceAB senses this stimulus and passes the signal on to the HK BceS (Dintner *et al.*, 2014). Upon autophosphorylation, BceS then activates its cognate RR BceR by phosphoryl-group transfer. Phosphorylated BceR will then bind to P_{bceA} and strongly induce *bceAB* transcription, ultimately resulting in increased BceAB production, thereby conferring AMP resistance (Mascher *et al.*, 2003, Ohki *et al.*, 2003, Bernard *et al.*, 2007, Rietkötter *et al.*, 2008, Fritz *et al.*, 2015) (Fig. 1 black system, BceAB not shown).

The main inducers of the Psd system are lipid II-binding lantibiotics such as nisin, actagardine, gallidermin and subtilin. In turn, the Psd system confers resistance against nisin, actagardine

and subtilin (Staroń *et al.*, 2011). The signal transduction pathway within Psd system (Fig. 1 grey system, PsdAB not shown) is similar to that described for the Bce system (Gebhard & Mascher, 2011). Despite significant sequence similarity between BceRS-BceAB and PsdRS-PsdAB, signaling in each system is generally well insulated from the other, although a previous study has demonstrated some degree of cross-phosphorylation between BceS and PsdR at high bacitracin concentrations (Rietkötter *et al.*, 2008) (Fig. 1, dotted arrow).

In bacteria, transcription initiation starts with promoter recognition by the σ subunit of the RNA polymerase holo-enzyme at the -35 promoter element, followed by binding and unwinding of the DNA double helix at the -10 promoter element (Lee *et al.*, 2012). A -10 promoter element with a perfect match to the σ^A consensus sequence (TATAAT) could be identified in P_{bceA}. It is located 6 bp upstream of the transcription initiation site, which is 32 bp upstream of the *bceA* start codon. However, a conserved -35 element was not found (Ohki *et al.*, 2003). An identical σ^A-dependent -10 element was also found in P_{psdA}, again lacking a clear -35 element at the appropriate position (Staroń *et al.*, 2011) (Fig. 2A). For such promoters deviating significantly from the consensus sequence at the -35 position, the σ subunit of RNA polymerase can still be recruited to these promoters by interaction with activators like RRs binding to the upstream region (Jarmer *et al.*, 2001, Paget & Helmann, 2003). RRs usually contain an N-terminal receiver domain and a C-terminal output domain. Both BceR and PsdR belong to the OmpR/PhoB subfamily of RRs with a C-terminal winged helix-turn-helix DNA-binding output domain that regulates the transcription of target genes by binding to their corresponding promoter regions via a specific recognition motif (Martínez-Hackert & Stock, 1997, Fabret *et al.*, 1999, Galperin, 2010). Inverted repeats on P_{bceA} as well as on P_{psdA} were mapped as BceR- and PsdR-binding sites, respectively, upstream of the corresponding -10 promoter elements (Fig. 2A), which implies an interaction between BceR-like RRs and the RNA polymerase holo-enzyme (Ohki *et al.*, 2003, de Been *et al.*, 2008, Staroń *et al.*, 2011).

The DNA binding domains of BceR and PsdR share 51% sequence identity (66% similarity) and the corresponding binding sites on P_{bceA} and P_{psdA} contain eleven out of fourteen identical nucleotides (Fig. 2A) (Joseph *et al.*, 2002). Nevertheless, no cross-regulation was detected at the transcriptional level between BceR-P_{psdA} and PsdR-P_{bceA} (Rietkötter *et al.*, 2008). Such a regulatory insulation, that is, prevention of nonspecific regulatory cross-talk, is of course desired and can arise at different molecular levels *in vivo* (Huynh & Stewart, 2011). The most prominent mechanism for conferring such signaling specificity depends on the molecular recognition between the two interaction partners (Podgornaia & Laub, 2013). However, in the case of the Psd and Bce systems, the high degree of identity between the two regulator binding sites raised the question how specificity can be ensured between two such closely related systems.

Here we provide detailed insights into the molecular mechanisms that ensure insulation and transcriptional regulation specificity between two Bce-like systems in *B. subtilis*, Bce and Psd at the level of RR-promoter interaction. Using both *in vivo* and *in vitro* approaches, we identified a secondary RR-binding site in both P_{bceA} and P_{psdA}, in addition to the previously identified (main) binding site. Importantly, we demonstrate that the main binding site, while being essential for promoter activation, does not significantly contribute to specificity of RR-promoter interactions. Instead, the secondary binding site and the variable linker region between the two sites are the primary specificity determinants. Moreover, our data show that *in vivo* promoter discrimination is based on competition between the two RRs for their respective binding sites.

Results

Identification of the minimal bceA *and* psdA *promoter motif*

P_{bceA} and P_{psdA} are the target promoters for the RRs BceR and PsdR, respectively (Staroń *et al.*, 2011). When *B. subtilis* is challenged with bacitracin, BceR is activated by the corresponding HK BceS and binds to a specific region of P_{bceA}, resulting in a strong upregulation of the operon encoding the ABC transporter for resistance (Mascher *et al.*, 2003) (Fig. 1). Previous work has already mapped an inverted repeat sequence for BceR binding in the P_{bceA} region (AAGCgTGTGACgaaaatGTCACAtGCTT) from -111 to -84 upstream of the *bceA* start codon (Ohki *et al.*, 2003). For P_{psdA}, a highly similar PsdR binding site (ATgTgACAgcatTGTaAgAT) could be identified from -99 to -80 upstream of the *psdA* start codon (Staroń *et al.*, 2011). In agreement with these studies, a comparative genomics study identified a putative binding site among most *bceA*-like promoters in Firmicutes bacteria, with an overall consensus sequence of TnACA-N_4-TGTAA as a recognition site for BceR-like RRs (Dintner *et al.*, 2011).

We first wanted to verify that these two known conserved binding motifs are indeed indispensable for the RR-dependent activation of the *bceA* and *psdA* promoters and identify the minimal regulatory elements for both promoter regions. Towards that goal, progressively truncated *bceA* promoters starting with the 5'-position ranging from -111 to -103 and ending at +82 relative to the ATG start codon of *bceA* were used to construct transcriptional *lacZ* reporter fusions (Table S2), which were integrated at the *amyE* locus in *B. subtilis* 168 wild type (WT) (Table S1). Progressively truncated *psdA* promoter fragments starting with 5'-positions ranging from -110 to -95, all ending at position +30 relative to the ATG start codon of *psdA*, were generated in a similar fashion (Fig. 2A). The promoter activity of the resulting reporter strains was determined by quantitative β-galactosidase assay in the presence of bacitracin (P_{bceA}) or nisin (P_{psdA}) (Staroń *et al.*, 2011).

Truncated *bceA* promoters from -111 until -106 showed activities comparable to the non-truncated promoter fragment starting at position -122 after bacitracin induction (black bars) (Fig. 2B). The truncations starting at position -105 and position -104 displayed a decreased promoter activity, while a further truncation of one additional nucleotide (starting at position -103) led to a complete loss of promoter activity after bacitracin induction.

Similar results were obtained for truncated *psdA* promoter fragments after nisin induction (grey bars) (Fig. 2C). No decrease of promoter activity was observed for truncations with 5'-positions starting from -110 to -100 relative to the positive control fragment, starting at position -126. The promoter activities were significantly reduced for fragments truncated at positions -99 to -96, while a truncation at position -95 led to a complete loss of activity after nisin induction.

These data confirmed that the 7-4-7 nt binding motif TGTGACGaaaaTGTCACA of P_{bceA} and the TGTGACAgcatTGTAAGA binding motif of P_{psdA} are indeed necessary for promoter induction and constitute likely binding sites for BceR and PsdR, in good agreement with previous reports (Ohki *et al.*, 2003, de Been *et al.*, 2008, Staroń *et al.*, 2011). These will be referred to as "main binding sites" (MBSs) from now on. Position -104 relative to *bceA* start codon and position -96 relative to *psdA* start codon determine the minimal 5'-end of active RR-dependent promoter fragments.

A secondary binding site on bceA *and* psdA *promoters*

Sequence analysis of P_{bceA} and P_{psdA} did not identify a typical -35 region (TTGACA) upstream of the -10 region as normally recognized by σ^A (Jarmer *et al.*, 2001). However, a 7 nt conserved half binding site for a BceR-like RR, located 13/14 nt downstream of the MBS and 38 nt upstream of the -10 region, was predicted for both the *bceA* and the *psdA* promoter regions (Dintner *et al.*, 2011). This observation implies the existence of a secondary binding site (SBS) instead of a typical -35 element on *bceA*-like promoters. Based on this prediction,

we annotated a putative SBS also showing the 7-4-7 pattern, as well as a linker region (L) between the MBS and the SBSs on both *bceA* and *psdA* promoters (Fig. 2A). We experimentally investigated the function of the predicted promoter motifs by randomizing their sequence, while maintaining the GC/AT content of the linker region. The fragments were used to generate *lacZ* reporter gene fusions (Tables 1+2) and were assayed as before.

Both the WT *bceA* promoter (Fig. 2D) and the *psdA* promoter (Fig. 2E) showed strong induction with the corresponding inducers bacitracin (black bars) or nisin (grey bars) compared to the non-induced samples (white bars), but no such response to the non-cognate inducer. The weak induction of P_{psdA} by bacitracin (Fig. 2E) was due to the known cross-phosphorylation of PsdR by BceS (Rietkötter *et al.*, 2008) (Fig. 1 dotted arrow). Randomizing the MBS led to a complete loss of activity for both promoters. The same effect was obtained when randomizing the sequence of the predicted SBS. However, activities of both *bceA* and *psdA* promoters only showed a slight decrease by randomly mutating the corresponding linker region (L) between the two binding sites (Fig. 2D and 2E).

The data demonstrate that on both P_{bceA} and P_{psdA}, a SBS exists that is located downstream of the MBS with a 13/14 nt linker region in between them. This SBS seemingly replaces the -35 region and is as indispensable as the MBS for RR-dependent promoter activity. Additional assays done by randomizing either the first or the second half of each SBS were in agreement with the results obtained for the completely randomized SBSs (data not shown), further demonstrating that each half binding site has the same importance for P_{bceA} and P_{psdA} activity.

Major specificity determinants are located in the region containing linker and SBS

So far, we have identified an extended regulatory region in P_{bceA} and P_{psA}, consisting of two binding sites, MBS and SBS, and a linker region between them. Since there is no cross-regulation at the RR-promoter interface, neither between BceR-P_{psdA} nor PsdR-P_{bceA} (Rietkötter *et al.*, 2008), we therefore wanted to analyse the specificity determinants within

196 the *bceA*/*psdA* promoters. Towards that goal, a series of chimeric promoters derived from
197 P_{bceA} and P_{psdA} was constructed (Table S2) and fused with *lacZ*. Chimeric promoters BP1-4
198 are derived from $P_{\underline{\mathbf{b}}ceA}$ (black) with gradually substituting $P_{\underline{\mathbf{p}}sdA}$ (grey) at the 3'-terminal end
199 (Fig. 3A). Chimeric promoters PB1-4 are derived from $P_{\underline{\mathbf{p}}sdA}$ (grey) with increasing of 3'-
200 fragments from $P_{\underline{\mathbf{b}}ceA}$ (black) (Fig. 3B). To specifically eliminate any cross-talk between the
201 Bce and Psd systems, the chimeric promoters as well as WT P_{bceA} and WT P_{psdA} fragments as
202 references, were introduced into the WT strain and additionally the otherwise isogenic
203 Δ*bceRS* (TMB1460) and the Δ*psdRS* (TMB1462) strains (Table S1). Compared to the WT
204 strain, the Δ*bceRS* and Δ*psdRS* backgrounds remove the effect of cross-phosphorylation and
205 hence provide a clearer view of individual RR-promoter interactions.
206 P_{bceA} showed the same high activity in the Δ*psdRS* mutant (Fig. 3D) as in the WT strain (Fig.
207 3C) after bacitracin induction, but no activity after nisin induction in either the WT (Fig. 3C)
208 or the Δ*bceRS* background (Fig. 3E). Correspondingly, P_{psdA} was highly induced by nisin in
209 both the WT strain (Fig. 3C) and the Δ*bceRS* mutant (Fig. 3E). Importantly, the moderate
210 induction of P_{psdA} by bacitracin seen in the WT (Fig. 3C) was not detected in the Δ*bceRS*
211 mutant (Fig. 3D) due to the elimination of cross-phosphorylation between BceS and PsdR.
212 These results are in agreement with previous studies that there is no cross-regulation at the
213 RR-promoter level.
214 Chimeric promoters BP1 and BP2 showed high activity after induction with bacitracin in both
215 the WT strain (Fig. 3C) and the Δ*psdRS* strain (Fig. 3D), but no activity upon nisin induction
216 in either the WT strain (Fig. 3C) or the Δ*bceRS* strain (Fig. 3E). Hence, BP2 could be
217 recognized by BceR, but not by PsdR. These results indicate that the specificity determinants
218 are located within the region upstream of and including the SBS. Interestingly, the chimeric
219 promoter BP3 could neither be induced by bacitracin in the Δ*psdRS* background (Fig. 3D) nor
220 by nisin in the Δ*bceRS* background (Fig. 3E), but showed moderate induction by bacitracin in
221 only the WT background (Fig. 3C). The observation that PB3 requires both TCSs for

222 responding to bacitracin might point towards the formation of RR heterodimers. But this
223 interpretation is purely speculative at the moment and will require follow-on studies.
224 Moreover, BP4 – possessing the whole region downstream of the MBS originating from P_{psdA}
225 – was not only moderately induced by bacitracin in the Δ*psdRS* background (Fig. 3D) but also
226 by nisin in the Δ*bceRS* background (Fig. 3E), indicating a relaxation of specificity from BceR
227 to PsdR. The results of BP2 and BP4 demonstrate that the major specificity determinants of
228 P_{psdA} are located in the region containing the linker and the SBS.
229 Chimeric promoters PB1 and PB2 showed a decreased activity after induction with nisin in
230 both the WT background (Fig. 3F) and the Δ*bceRS* mutant (Fig. 3G) relative to P_{psdA}, and no
231 bacitracin induction in the Δ*psdRS* mutant (Fig. 3H), indicating no change of specificity.
232 These results corroborate that the region downstream of the SBS is not relevant for the RR-
233 promoter specificity. Interestingly, PB3 showed a significantly decreased activity in the
234 Δ*bceRS* mutant with nisin induction (Fig. 3G) and a strongly increased activity in the Δ*psdRS*
235 mutant with bacitracin induction (Fig. 3H). Chimera PB4 was not inducible by nisin in the
236 Δ*bceRS* strain (Fig. 3G), but instead showed high induction by bacitracin in the Δ*psdRS* strain
237 (Fig. 3H), strongly reminiscent of the intact P_{bceA}. The promoter activities of PB3 and PB4 in
238 the WT strain (Fig. 3F) were in accordance with those observed in both mutant backgrounds.
239 These data indicate that the change of specificity from P_{psdA} to P_{bceA} can be achieved by
240 exchanging the SBS (PB3), and is further strengthened by an additional substitution of the
241 linker region (PB4).
242 The analysis of chimeric promoter constructs described above demonstrates that (i) all three
243 regulatory parts (MBS-linker-SBS) together determine the RR-specificity, with (ii) the region
244 downstream of the MBS of P_{bceA}/P_{psdA}, containing the linker and the SBS, functioning as the
245 main discriminator for BceR/PsdR recognition.
246

Rewiring the specificity between P_{bceA} and P_{psdA} enables dissecting the roles of individual specificity determinants

To further investigate the functions of MBS, linker region and SBS on the *psdA* promoter for PsdR recognition, additional chimeric promoters were generated with different combinations of these three motifs on P_{bceA} replaced by the corresponding region of P_{psdA} (Fig. 4A) to rewire specificity from BceR to PsdR. Promoter activities were measured as described above in the WT strain (Fig. 4C), the Δ*psdRS* strain (Fig. 4D) and the Δ*bceRS* strain (Fig. 4E).

Compared to P_{bceA}, replacing only the MBS (M), the linker (L) or both (M+L) of P_{bceA} with the corresponding region of P_{psdA} showed decreased promoter activity in the WT strain after induction with bacitracin (Fig. 4C) as well as in the Δ*psdRS* mutant (Fig. 4D). No increase of the promoter activity after induction by nisin was observed in either the WT strain (Fig. 4C) or the Δ*bceRS* mutant (Fig. 4E). This indicates that the MBS, the linker or both of P_{psdA} are not enough to cause activation via PsdR. Changing the SBS (S) on P_{bceA} into P_{psdA} led to a decrease of promoter activity after induction with bacitracin in the WT strain (Fig. 4C) as well as in the Δ*psdRS* mutant (Fig. 4D) and a slight but detectable increase of promoter activity after induction with nisin in the Δ*bceRS* mutant (Fig. 4E). This indicates that exchanging only the SBS alone already conferred a relaxation of promoter specificity from BceR to PsdR.

Substitution of the linker together with the SBS (L+S) resulted in a higher promoter activity compared to only exchanging the SBS (S) both after bacitracin induction (Fig. 4D) and nisin induction (Fig. 4E). This indicates that the linker region (L) can enhance promoter activity with both cognate PsdR and noncognate BceR. Compared to only the SBS switch (S), exchanging both the MBS and the SBS simultaneously (M+S) resulted in a severe decrease of the promoter activity after induction with bacitracin (Fig. 4D), while causing an increase of the promoter activity after induction with nisin (Fig. 4E).

Taken together, these results suggest that the SBS on P_{psdA} is the main discriminator for PsdR-binding to P_{psdA}, even though the intensity of induction with the SBS substitution alone is not

very strong. The linker cannot determine specificity by itself but can increase promoter activity with both BceR and PsdR, which explains the change of specificity that was detected for construct BP4 including the linker and the SBS but not for construct BP3 with only the SBS (Fig. 3C). Despite the fact that the MBS is absolutely crucial for RR-promoter interaction, the MBS of P_{psdA} alone cannot determine specificity. Instead, it supports the SBS in strengthening the promoter activity. Not surprisingly, switching all three elements together (M+L+S) resulted in the highest change of specificity after induction with nisin (Fig. 4E), demonstrating that all three parts together contribute to the specificity.

In order to support the results obtained above, a similar approach was performed towards rewiring the specificity from P_{psdA} to P_{bceA}. A comparable series of chimeric promoters with different combinations of the MBS, the linker region and the SBS of P_{psdA} being replaced by the corresponding regions from P_{bceA} was constructed (Fig. 4B) (Table S2) and the promoter activities of the corresponding *B. subtilis* reporter strains (Table S1) were determined. The results are shown in Fig. 4F-4H. Overall, the combined data is in very good agreement with the results obtained for rewiring the specificity from P_{psdA} to P_{bceA} with only minor differences between the two sets.

Taken together, exchanging the MBS alone had no effect on the specificity of induction of P_{bceA} and only caused a very minor change in P_{psdA} behaviour. Instead, the SBS provides the major discriminator for RR binding. The data is particularly clear for the BceR-P_{bceA} interaction, where exchange of the SBS alone was able to cause a clear change in specificity, while the role of the SBS of P_{psdA} for the PsdR-P_{psdA} pair is less prominent. Both promoters have in common that the MBSs strengthen the specificity by increasing the interactions with the cognate RR, while simultaneously reducing the interactions with the non-cognate RR. In addition, the linker regions fine tune promoter activity. While specific roles can therefore be attributed to these three regulatory elements, it should be pointed out that the specificity of

BceR-like RRs for their target promoters is ultimately determined by the specific combination of MBS, linker and SBS working together.

In vitro *analysis of BceR binding to* P_{bceA} *and* P_{psdA}

Next, we wanted to investigate if BceR could also discriminate between its native promoter P_{bceA} and the non-cognate P_{psdA} *in vitro*. BceR carrying an N-terminal His_{10}-tag with the expected molecular mass of about 27 kDa was produced in and purified from the cytoplasmic fraction of *E. coli* C43(DE3) cells containing plasmid pCF120 (Table S2). Electrophoretic mobility shift assays (EMSAs) were performed with purified BceR and the two promoters P_{bceA} and P_{psdA}. 300 bp promoter DNA fragments (300 bp) of P_{bceA} or P_{psdA} containing the MBS, the linker region and the SBS were amplified and labeled at the 5'-end with 6FAM by PCR. 6FAM labeled P_{sigW} (the target promoter of an ECF sigma factor in *B. subtilis*) was used as a negative control.

The results of EMSAs with BceR and P_{bceA} are shown in Figure 5A. Increasing concentrations of BceR phosphorylated by the addition of phosphoramidate (BceR-P; see Experimental procedure) were incubated with 30 fmol of 6FAM-P_{bceA} (lane 2 to lane 5), demonstrating a concentration-dependent binding of BceR-P to P_{bceA}. The first shift was observed at 1.0 µM BceR-P representing the initial binding event of BceR-P to P_{bceA}. An additional shift occurred at BceR-P concentrations of 1.5 µM or above and presumably represents a second binding event, consistent with the presence of two BceR binding sites on the DNA fragment. In contrast, unphosphorylated BceR showed a much weaker binding (data not shown), which demonstrated that RR-phosphorylation promotes DNA binding by increasing BceR affinity to P_{bceA}.

EMSAs were also performed between BceR-P and P_{psdA} (Fig. 5B). Two successive shifts of P_{psdA} band in lane 3 and lane 4 compared to free P_{psdA} DNA fragment (lane 1) demonstrated that BceR-P can also bind to two sites in the noncognate but highly related P_{psdA} *in vitro*. In

contrast, no shift was observed for the P_{sigW} DNA fragment (Fig. 5E), confirming the overall specificity of the assay: BceR-P cannot bind to promoter fragments that do not harbor the binding motifs of a P_{bceA}-like promoter.

To further illustrate the specificity and affinities of BceR-P binding to P_{bceA} and P_{psdA}, 900 fmol of unlabeled promoter fragments were used as competitor DNA (Fig. 5A/5B lane 6-8). Co-incubation of BceR-P with 30 fmol 6FAM-P_{bceA} and 900 fmol unlabeled P_{bceA} fragment (Fig. 5A lane 6) completely abolished the retardation of the labeled P_{bceA} fragment due to the competitive binding of BceR-P to an excess of unlabeled P_{bceA}. However, the shift of 6FAM-P_{bceA} band was not influenced by adding a 30-fold molar excess of unlabeled P_{psdA} (Fig. 5A lane 7) or P_{sigW} (Fig. 5A lane 8). This shows that despite its ability to bind to both P_{bceA} and P_{psdA} in isolation, BceR is clearly able to distinguish between the two promoters and preferentially binds to its cognate target. In contrast, the retardation of the 6FAM-P_{psdA} DNA fragment was abolished by either addition of 30-fold excess unlabeled P_{bceA} (Fig. 5B lane 6) or unlabeled P_{psdA} (Fig. 5B lane 7) fragments but not by P_{sigW} (Fig. 5B lane 8). These results clearly demonstrate that, while BceR-P can interact with seemingly identical activities with both target promoters in isolation (the shift occurs at comparable BceR-P concentrations), it preferentially binds to its native promoter, P_{bceA}, compared to P_{psdA} *in vitro* when incubated in competition. Hence, the binding affinity for its cognate target promoter P_{bceA} seems to be higher than for P_{psdA}, which determines the *in vivo* specific transcription initiation. Unfortunately, any efforts to purify PsdR failed, thereby preventing the performance of similar *in vitro* studies on PsdR-P_{psdA}/P_{bceA} interactions.

Cooperative binding of BceR to two binding sites on $\mathbf{P_{bceA}}$

The *in vivo* promoter activity assays demonstrated that both binding sites on P_{bceA} are indispensable for BceR-P_{bceA} interaction (Fig. 2D). Moreover, the EMSA studies on complete promoter fragments strongly suggest two binding events at P_{bceA} *in vitro* (Fig. 5A). To

discriminate between the individual binding reactions, we next performed EMSAs with BceR-P on 6FAM labeled *bceA* promoter DNA-fragments carrying randomized versions of either the MBS or the SBS (Fig. 5D).

Incubation of BceR-P with labeled P_{bceA} SBS^R (P_{bceA} containing a native MBS and a randomized and hence inactive SBS) caused only a single shift at a BceR-P concentration of 1.0 µM (Fig. 5C), a concentration comparable to the threshold concentration for binding to the intact P_{bceA} fragment (Fig. 5A lane 3). Increasing the BceR-P concentration did not lead to any additional shift. Hence, P_{bceA} containing only the MBS merely allows one binding event, which is the binding of BceR-P to the MBS. The identical BceR-P concentrations required for shifting either the WT or the SBS^R fragments indicates that binding of BceR-P to the MBS is independent of the SBS.

Incubation of BceR-P with labeled P_{bceA} MBS^R (P_{bceA} containing a randomized and hence inactive MBS but an intact SBS) failed to retard the DNA-fragment within the same concentration range (Fig. 5D). This suggests that either BceR-P has a very low affinity for binding to the SBS alone or that binding to the SBS depends on and occurs after BceR-P binding to the MBS.

Determination of binding kinetics of BceR-promoter interaction unravels the mechanism that determines BceR promoter specificity

For quantitatively describing the binding kinetics of BceR-promoter interactions, we next performed SPR spectroscopy in combination with Interaction Map® (IM) analysis. We captured a biotin-labeled DNA-fragment comprising the P_{bceA} region (see Table S3 for exact sequence) to a sensor chip coated with immobilized streptavidin. Next, increasing concentrations of His_{10}-BceR and His_{10}-BceR-P were injected over the chip surface. While non-phosphorylated BceR did not interact with the P_{bceA} promoter (Fig. 6A), BceR-P showed clear binding (Fig. 6B). Since BceR has two binding sites on the DNA-fragment used for SPR,

we performed IM analyses. In order to determine and quantify the individual binding events represented by the SPR curves. Briefly, the IM algorithm splits the experimental SPR data set into several theoretical monovalent binding events and selects the binding curves that best fit the experimental data when summed up. By plotting the association rate k_a and the dissociation rate k_d within a two-dimensional distribution, heterogeneous binding data can be displayed as a map, in which each peak corresponds to one component that contributes to the cumulative binding curve (Altschuh *et al.* 2012). The sensorgram could be split into two binding events, one characterized by a fast ON/fast OFF (k_a=1.8 × 10^6/M*s; k_d=1.0x10^{-1}/s) and one characterized by a slow ON/slow OFF binding kinetics (k_a=3.2 × 10^5/M*s; k_d=5.5x10^{-4}/s) that differ in their overall affinity (K_D=58 nM and K_D=1.7 nM, respectively) (Fig. 6E). Each binding peak makes up an approximate peak weight of 50% revealing that both DNA-binding sites are bound by equal amounts of BceR-P molecules.

As a next step, we determined the binding kinetics between BceR-P and P_{bceA} when the MBS or the SBS was randomized (MBS^R or SBS^R, respectively). Inactivation of the MBS completely prevented DNA-binding of BceR-P (Fig. 6C), while a clear DNA-binding of BceR could still be observed when only the SBS was randomized (Fig. 6D). In contrast to the sensorgram including both intact binding sites (Fig. 6B), the IM of the corresponding sensorgram suggested in principle only the slow ON/slow OFF binding event (k_a=1.5 × 10^6 M*s; k_d=4.9 × 10^{-4}/s, resulting in an overall binding affinity of K_D=0.4 nM (Fig. 6F). However, the *in silico* sensorgram is comparable to that one of the slow ON/slow OFF interaction of BceR-P to intact P_{bceA} site revealing that this reflects binding of BceR-P to the MBS although the overall affinity is approximately six-fold higher, mainly caused by the five-fold higher ON rate. The peak weight is calculated as 80%, meaning that this interaction mainly contributes to the measured sensorgram. However, the fast ON/fast OFF peak did not completely disappear, but compared to the intact promoter site the peak weight is lower than 20% and can therefore be neglected. These data clearly show that the MBS of the P_{bceA} region

is essential for binding of the RR to the DNA. Moreover, the affinity of the RR is not sufficient to allow any binding of BceR to the SBS if the MBS was not previously occupied, at least under the experimental regime applicable for SPR spectroscopy. Comparing the binding kinetics of BceR-P to the intact and the SBS^R promoter, it can be assumed that the SBS increases the overall affinity of the RR to the promoter region, and therefore is important for triggering gene expression.

Finally, we wondered if the binding mechanism of BceR-P is also similar to the related P_{psdA}. We captured DNA comprising the P_{psdA} promoter as well as the P_{psdA} promoter in which the MBS or SBS were inactivated (MBS^R or SBS^R, respectively) onto the chip. First, we injected increasing concentrations of non-phosphorylated BceR over the chip and observed, as expected, no binding to the P_{psdA} promoter (Fig. 6G). Then, increasing concentrations of BceR-P were injected. The interaction of Bce-R to P_{psdA} was almost comparable to the one observed for the P_{bceA} promoter (Fig. 6H). The IM analysis underlying this sensorgram also revealed two binding events, one with fast ON/fast OFF ($k_a=6.2 \times 10^5$/M*s; $k_d=1.2x10^{-1}$/s) and one with slow ON/slow OFF binding kinetics ($k_a=1.1 \times 10^5$/M*s; $k_d=6.2x10^{-4}$/s) likewise resulting in two binding events that differ in their overall affinity (K_D=188 nM and K_D=6.2 nM, respectively). Compared to the affinities of BceR-P to P_{bceA}, the binding affinities for P_{psdA} are indeed in a similar range, but both P_{psdA} binding sites differ in their affinity in the factor of three to BceR-P (Fig. 6L). In agreement with the data obtained for the P_{bceA} promoter region, inactivation of the MBS completely prevented BceR-P binding to the P_{psdA} promoter region (Fig. 6I). Inactivation of the SBS showed a 1:1 interaction described by one peak in the IM analysis that corresponds to the slow ON/slow OFF MBS site with an association rate of $k_a=1.1 \times 10^5$ M*s and a dissociation rate $k_d=7.3 \times 10^{-4}$/s making an overall binding affinity of K_D=6.7 nM (Fig. 6M), also fitting well to k_a, k_d, and K_D of the BceR-P/P_{psdA} interaction (Fig. 6L). These data clearly demonstrate that the binding mechanism of BceR-P to the P_{psdA}

promoter is comparable to that of BceR-P to the P_{bceA} promoter, however, with slightly altered binding kinetics and binding affinities differing by a factor of three.

Taken together, the *in vitro* data obtained for the binding of BceR-P to isolated promoter fragments by EMSA (Fig. 5A/B) and SPR spectroscopy (Fig. 6B/E and Fig. 6 H/L) are in good agreement with each other. They indicate a hierarchical cooperative binding of phosphorylated BceR-like RRs first to the MBS and then to the SBS. While promoter discrimination could not be explained by EMSAs alone, we could determine slight differences in the binding affinities by SPR combined with IM analyses that could explain promoter preference and discrimination of isolated RRs on single promoter fragments and therefore selected activation of transcription. Moreover, DNA curvature as well as interaction of BceR-P with the RNA polymerase could be further factors that finally lead to total promoter activation *in vivo*.

Discussion

On P_{bceA} and P_{psdA}, no typical -35 element was found in the appropriate location upstream of the -10 element, indicating that the σ unit of the RNA polymerase cannot bind properly to the promoter by itself to initiate transcription initiation. However, binding can nevertheless be established under such conditions when the σ unit interacts with an RR that binds to upstream elements of the promoter, thereby compensating weak σ unit binding (Lee *et al.*, 2012). DNA binding domain structures of both PhoB and OmpR from the OmpR subfamily showed that these RRs can directly interact with the σ subunit of the RNA polymerase (Martínez-Hackert & Stock, 1997, Blanco *et al.*, 2002). BceR and PsdR, which belong to the same subfamily, are assumed to assist the transcription initiation of RNA polymerase in a similar way.

Specific transcription initiation by RRs is important for maintaining the insulation of the corresponding signaling systems. The similarity of Bce-like RRs DNA-binding domain and their binding sites on target promoters increases the potential of unwanted cross-talk at the transcription initiation level. However, we could show that Bce-type RRs in *B. subtilis* are extremely specific in inducing the transcription of only their cognate ABC transporter operons. While we observed binding of BceR-P to both the cognate P_{bceA} and the non-cognate P_{psdA} with very similar affinities *in vitro* (Fig. 5A and 5B), BceR can only induce the transcription of *bceAB* but not of *psdAB in vivo* (Fig. 3). Moreover, our EMSA experiments showed that when incubated with a mixture of both promoter fragments, BceR is able to specifically bind its cognate target, even if that is present at 30-fold lower concentrations (Fig. 5). Promoter discrimination between cognate and non-cognate binding sites can therefore be based on even minor differences in binding affinities of isolated RRs to the otherwise highly similar binding sites, as demonstrated by the SPR measurements (Fig. 6). This discriminatory ability becomes especially apparent under conditions of competition between binding partners (as shown by the EMSA competition experiments, Fig. 5), which is most reminiscent of the intracellular environment, where both RRs and DNA target sequences are present at the same time.

The slight affinity preference is the ability of the RR to distinguish the cognate from non-cognate promoter in the natural cellular setting. Our data strongly suggest that *B. subtilis* evolved a sophisticated mechanism to maintain this ability by combining this existing target site competition of homologous RRs to their respective binding sites with hierarchical and cooperative DNA binding (Fig. 7). Instead of the single binding sites reported previously (Ohki *et al.*, 2003, de Been *et al.*, 2008), we experimentally demonstrated the presence of two binding sites in the regulatory region of the Bce-type RR target promoters (Fig. 2D and 2E), as was already suggested by a comparative genomics study on Bce-like TCSs (Dintner *et al.*, 2011). By performing EMSAs and SPR assays of BceR with P_{bceA} mutants carrying random mutation in either the MBS or the SBS, we demonstrated that BceR has a high affinity and

shows independent binding to the upstream MBS (Fig. 5C and 6D). BceR has a low affinity for the downstream SBS and cannot bind to it alone under our experimental conditions (Fig. 5D and 6C). While it is not possible to unequivocally determine the order of BceR binding to its two target sites from the data presented herein, our results nevertheless strongly suggest that a BceR dimer first binds to the high-affinity MBS. This first binding event might then assist the subsequent binding of another dimer to the downstream low-affinity SBS. In this, binding to the MBS appears to be of low specificity, while the second binding event to the SBS occurs with high specificity. This is supported by our *in vivo* promoter activity assays where we showed that exchanging the SBS between the P_{bceA} and P_{psdA} fragments resulted in a much stronger influence on promoter specificity than exchanging the MBS by *in vivo* promoter activity assays (Fig. 4). This hierarchical and cooperative binding to the two sites enables BceR to discriminate between its cognate promoter P_{bceA} and the non-cognate P_{psdA}, which is based on: (i) The MBSs of these two promoters differ only in three bases and provide a high-affinity, low-specificity docking site; (ii) The SBSs of these two promoters harbor five different bases and represent low-affinity, yet high specificity interaction sites; (iii) Only this combination of MBS and SBS together with the binding competition described above ultimately allows BceR-P to discriminate between the cognate promoter P_{bceA} and the non-cognate P_{psdA}, thereby ultimately ensuring the wiring specificity of highly similar RRs.

It should be pointed out that the specificity of interaction between BceR and the MBS/SBS of either the cognate or non-cognate site – as expressed by the different binding affinities determined by SPR measurement *in vitro* (Fig. 6) – will *in vivo* of course be influenced by the relative cellular concentrations of phosphorylated BceR-like RRs. For both P_{bceA} and P_{psdA}, the K_D values differ by a factor of 30 between the MBS and the SBS, with the first in the range of 2-7 nM while the latter was determined in the 50-150 nM range (Fig. 6).

The strong discriminatory power of the SBS relative to the MBS suggests cellular BceR-P concentrations in the medium (approx. 10 to 100) nanomolar range. Under such conditions,

the MBS of both P_{bceA} and P_{psdA} would be fully bound, while the small differences in binding affinities to the respective SBS should be sufficient for promoter discrimination at RR concentrations near the K_D values. Unfortunately, no data on the cellular concentrations of BceR-like RRs is available, and even a comprehensive quantitative analysis aimed at determining the cellular amounts of all mRNA and protein species of the *B. subtilis* cell failed to detect BceR in any of over 200 conditions tested (Buescher et al. 2012) indicative of a very low basal abundance. The true physiological conditions for promoter-RR interaction therefore have to remain speculative.

The linker regions of these two promoters showed characteristically distinct GC/AT contents: P_{bceA} has a high AT content, while P_{psdA} has a high GC content (Fig. 2A). We showed that mutating the linker region into a random sequence while maintaining the GC/AT content of each promoter only slightly affected the promoter activity (Fig. 2D and 2E). However, exchanging the linker region between these two promoters, which means changing the GC/AT content, resulted in a more pronounced effect on the promoter activity (Fig. 4). AT-rich sequences are known to mediate DNA bending (Koo *et al.*, 1986). One possibility is that the AT-rich linker region on P_{bceA} confers a structural difference compared to P_{psdA} by bending the promoter between two binding sites, which might accommodate the binding of two BceR dimers.

The high specificity of the SBS is presumably determined mainly by its first half-site, for which P_{bceA} and P_{psdA} differ in four out of seven bases. In contrast, the second half-sites of the SBSs only differ in one base. The sequence identity of the second half-site and its location at the -35 position suggests that it can probably be bound by both BceR and the σ^A subunit of the RNA polymerase. Along those lines, we saw that a P_{bceA} mutant with the SBS replaced by a second MBS (MBS-linker-MBS) completely lost its promoter activity (data not shown), further supporting the importance of the second half for transcription initiation, presumably by σ^A subunit binding. Alternatively, the binding of the σ^{70} subunit to the -35 element could

be replaced by protein-protein interactions between the RNA polymerase and BceR/PsdR. Such a mechanism was shown *in vitro* for PhoB and CRP dependent promoter activation. (Kumar *et al.*, 1994). A recent study demonstrated that in PhoB regulated promoters, σ^{70} forms a number contacts with DNA-bound PhoB, replacing contacts with the -35 element (Blanco *et al.*, 2011).

Hierarchical and cooperative DNA binding is widespread among the OmpR RR subfamily. For example, PhoB can bind cooperatively to two binding sites in the *pstS* promoter with different individual binding affinities (Blanco *et al.*, 2012). P_{ompF} has three OmpR binding sites with gradually reduced affinity from upstream to downstream, and binding of OmpR to the first site is important for subsequent binding to the lower-affinity downstream sites (Harlocker *et al.*, 1995). Likewise, the RR YpdB from *E. coli* also shows a two-step cooperative binding mechanism to its target promoter P_{yhjX} (Behr *et al.*, 2016): binding of YpdB to the upstream site A initiates subsequent binding to the downstream site B followed by a rapid and successive promoter clearance. Similar to P_{bceA}-binding of BceR, binding of YpdB to P_{yhjX} was completely abolished if site A was inactivated (Behr *et al.*, 2016).

Interestingly, highly cooperative binding of BceR-P to its target promoter was already strongly suggested by a recent quantitative study on the regulatory dynamics of the Bce system (Fritz *et al.*, 2015). This study indicated a high degree of cooperativity within the signaling pathway, presumably caused by cooperative binding of BceR-P to multiple sites in the target promoter. This cooperativity was shown to be crucial for the highly dynamic dose-response behavior of *bceAB* expression in the presence of increasing amounts of bacitracin, resulting in an accurate produce-to-demand strategy that adjusts cellular BceAB levels to just the right amount to cope with the current presence of bacitracin (Fritz *et al.*, 2015). These specific results on BceR cooperativity are in good agreement with a recent theoretical study, which identified cooperativity as an important mechanism to significantly reduce crosstalk in gene regulation (Friedlander *et al.*, 2016).

The evolution of such complex regulatory mechanisms often correlates with the regulatory function of the RRs: e.g. PhoB and OmpR regulate dozens of operons in *E. coli* in the presence of certain stimuli. Some of these operons need to be highly upregulated while others require only moderate or subtle modulations in response to a given trigger. Controlling such differential expression levels of multiple target operons by a single RR can be achieved through assembly of different numbers of binding sites with sequence variations. We have demonstrated for *B. subtilis* that a similar mechanism can also be used to maintain signaling specificity and regulatory insulation between paralogous Bce-like systems that presumably evolved by gene duplications followed by sequence diversification of both the DNA binding domain and their target promoter sequence. Combining a high-affinity but low-specificity MBS and a high-specificity but low-affinity SBS provides *B. subtilis* with enough sequence space to ensure that Bce-like RRs can evolve the ability to discriminate cognate from non-cognate promoters, thereby ensuring the signaling fidelity of highly paralogous Bce-like systems on the transcription level. It will be interesting to see if such a combination of competitive and hierarchical cooperative binding can also explain the target site discrimination for other paralogous pairs of two-component systems.

Experimental procedures

Bacterial strains and growth conditions. All strains used in this study are listed in Table S1. *E. coli* DH5α and XL1-blue were used for cloning. All *B. subtilis* strains used in this study are derivatives of the laboratory WT strain 168. *E. coli* and *B. subtilis* were grown routinely in Luria-Bertani (LB) medium at 37°C with aeration. *B. subtilis* was transformed by natural competence as previously described (Harwood & Cutting, 1990). Ampicillin (100 µg ml^{-1}) was used for selection of all plasmids in *E. coli*. Chloramphenicol (5 µg ml^{-1}), spectinomycin (100 µg ml^{-1}) or erythromycin (1 µg ml^{-1}) plus lincomycin (25 µg ml^{-1}) for macrolide-

lincosamide-streptogramin B (mls) resistance were used for the selection of *B. subtilis* mutants. Bacitracin was supplied as the Zn^{2+}-salt. Growth was measured as optical density at 600 nm wavelength (OD_{600}). Solid media contained 1.5 % (w/v) agar.

Plasmid construction and genetic techniques. All plasmids constructed in this study are listed in Table S2. The corresponding primer sequences are provided in the supplemental material (Table S3). Different promoter fragments derived from P_{bceA} and P_{psdA} were fused to *lacZ* and cloned into the vector pAC6 (Stülke *et al.*, 1997) via the EcoRI/BamHI sites. The details of all promoter constructs are given in Table S2. For construction of the BceR-production plasmid in *E. coli*, *bceR* was amplified with primers TM2007/2008 and cloned into vector pET16b with XhoI and BamHI obtaining pCF120, resulting in an N-terminal His_{10}-tag fusion. Constructs for unmarked gene deletion in *B. subtilis* were cloned into the vector pMAD (Arnaud *et al.*, 2004). For each operon to be deleted, 800-1000 bp fragments located immediately before the start codon of the first gene ("up" fragment) and after the stop codon of the last gene ("down" fragment) were amplified. The primers were designed to create a 17-20 bp overlap between the PCR-products (Table S2), facilitating fusion of the fragments by PCR overlap extension and subsequent cloning into pMAD. Gene deletions were performed as previously described (Arnaud *et al.*, 2004). All constructs were checked for by sequencing, and all *B. subtilis* strains created were verified by colony PCR using appropriate primers.

β-Galactosidase assays. Promoter activity assays were performed as described previously (Mascher *et al.*, 2004). In brief, cells were inoculated from fresh overnight cultures and grown in LB medium at 37°C with aeration until they reached an OD_{600} between 0.4 and 0.5. The cultures were split into 2 mL aliquots and challenged with 30 µg ml^{-1} bacitracin or 2 µg ml^{-1} nisin with one aliquot left untreated (non-induced control). After incubation for an additional 30 min at 37°C with aeration, the cultures were harvested and β-galactosidase activities were determined as described previously, with normalization to cell density (Miller, 1972).

Overproduction and purification of His-tagged BceR. To produce BceR carrying an N-terminal His_{10}-tag, *E. coli* C43 (DE3) cells harboring plasmid pCF120 were grown at 25 °C with agitation until they reached an OD_{600} of about 0.4. IPTG (0.5 mM) was added to the culture and incubation was continued at 18 °C with agitation overnight. Cells were harvested by centrifugation at 4,400 × g for 10 min. The cell pellet was washed with buffer A (20 mM potassium phosphate buffer [pH7.5], 100 mM NaCl) and stored at -20 °C until use.

To purify His_{10}-tagged BceR, cells were resuspended in buffer B (50 mM potassium phosphate buffer [pH 7.5], 500 mM NaCl, 5 mM β-mercapto-ethanol, 10 mM imidazole and 10 % (w/v) glycerol) supplemented with 0.1 mM phenylmethylsulfonyl fluoride (PMSF) plus 2 mg DNaseI and disrupted by three passages through a French pressure cell (Thermo Fisher) at 20,000 PSI. Unbroken cells were removed by centrifugation at 17,000 × g for 20 min and the cell-free supernatant was filtered through a 0.45 µm syringe filter before loading onto a 1 ml Ni^{2+}-NTA resin column (Qiagen) pre-equilibrated with 5 column volumes (CVs) of buffer B. Loading was followed by washing with 5 CVs of buffer B and then with 5 CVs of buffer B containing 100 mM imidazole. BceR was eluted with buffer B supplemented with 250 mM imidazole. Fractions containing BceR were pooled and dialyzed in buffer C (50 mM Tris-HCl [pH 7.5], 150 mM NaCl, 10 mM $MgSO_4$, 5 mM β-mercapto-ethanol, 5 mM imidazole and 10 % (w/v) glycerol) at room temperature for 1 h. Protein concentration was determined with Roti®-Nanoquant (Carl Roth), and the proteins stored at 4 °C until use.

Electrophoretic Mobility Shift Assays (EMSA). For electrophoretic mobility shift assays, different DNA fragments (around 300bp) generated by PCR using primers TM3146 (5' terminal 6FAM labeled) and TM3137 were purified by gel extraction. Unlabeled DNA fragments were generated by PCR using primers TM3136/3137 and purified by gel extraction. N-terminal His_{10}-BceR samples in the non-phosphorylated state and after phosphorylation with 50 mM phosphoramidate at room temperature for 2 h were centrifuged at 16,060 × g and

4 °C for 10 min to remove the aggregated protein. Protein concentrations of the supernatants were determined as above and the proteins were stored on ice. Binding reactions were set by incubating 6FAM-labelled DNA-fragments with different concentrations of His_{10}-BceR at room temperature for 20 min. The reaction mixture included 30 fmol labeled target DNA and 0, 0.5, 1.0, 1.5, 2.0 µM protein with binding buffer (20 mM Tris-HCl [pH 7.5], 50 mM KCl, 10 mM $MgSO_4$, 1 mM DTT, 5 µg ml^{-1} salmon sperm DNA and 4 % (w/v) glycerol) in a total volume of 5.5 µl. Unlabeled competitor DNA was added to the system to a final concentration of 900 fmol. Samples were loaded on a 6% native polyacrylamide gel and electrophoresis was performed by 300 V for 15 min in 1× TBE buffer. 6FAM fluorescence of labeled DNA bands was detected by PhosphorImager (Typhoon Trio™, GE Healthcare).

Surface Plasmon Resonance (SPR) spectroscopy. SPR assays were performed in a Biacore T200 using carboxymethyl dextran sensor chips pre-coated with streptavidin (Xantec SAD500-L, XanTec Bioanalytics GmbH, Düsseldorf, Germany). All experiments were carried out at a constant temperature of 25°C and using HBS-EP+ buffer [10 mM HEPES pH 7.4; 150 mM NaCl; 3 mM EDTA; 0.05 % (v/v) detergent P20] as running buffer. Before immobilizing the DNA fragments, the chips were equilibrated by three injections using 1 M NaCl/50 mM NaOH at a flow rate of 10 µl min^{-1}. Then, 10 nM of the respective double-stranded biotinylated DNA fragment was injected using a contact time of 420 sec and a flow rate of 10 µl min^{-1}. As a final wash step, 1 M NaCl/50 mM NaOH/50% (v/v) isopropanol was injected. Approximately 100-200 RU of each respective DNA fragment were captured onto the respective flow cell. All interaction kinetics of BceR or BceR-P with the respective DNA fragment were performed in HBS-EP+ buffer at 25°C at a flow rate of 30 µl min^{-1}. The proteins were diluted in HBS-EP+ buffer and passed over all flow cells in different concentrations (0.1 nM-10 nM) using a contact time of 180 sec followed by a 300 sec dissociation time before the next cycle started. After each cycle the surface was regenerated

by injection of 2.5 M NaCl for 60 sec at 30 µl min^{-1} flow rate followed by a second regeneration step by injection of 0.5% (w/v) SDS for 60 sec at 30 µl min^{-1}. All experiments were performed at 25°C. Sensorgrams were recorded using the Biacore T200 Control software 2.0 and analyzed with the Biacore T200 Evaluation software 2.0. The surface of flow cell 1 was not immobilized with DNA and used to obtain blank sensorgrams for subtraction of bulk refractive index background. The referenced sensorgrams were normalized to a baseline of 0. Peaks in the sensorgrams at the beginning and the end of the injection emerged from the runtime difference between the flow cells of each chip.

Calibration-free concentration analysis (CFCA) was performed using a 5 µM solution of purified BceR-P (calculated from Lowry-based protein determination), which was stepwise diluted 1:2, 1:5, 1:10, and 1:20. Each protein dilution was two-time injected, one at 5 µl min^{-1} as well as 100 µl min^{-1} flow rate. On the active flow cell P_{psdA}-DNA was used for BceR-P-binding. CFCA basically relies on mass transport, which is a diffusion phenomenon that describes the movement of molecules between the solution and the surface. The CFCA therefore relies on the measurement of the observed binding rate during sample injection under partially or complete mass transport limited conditions. Overall, the initial binding rate (dR/dt) is measured at two different flow rates dependent on the diffusion constant of the protein. The diffusion coefficient of BceR-P was calculated using the Biacore diffusion constant calculator and converter webtool (https://www.biacore.com/lifesciences/Application_Support/online_support/Diffusion_Coefficient_Calculator/index.html), whereby a globular shape of the protein was assumed. The diffusion coefficient of BceR-P was determined as $D=1.031x10^{-10}$ m^2/s. The initial rates of those dilutions that differed in a factor of at least 1.5 were considered for the calculation of the „active“ concentration, which was determined as $5x10^{-8}$M (1% of the total protein concentration determined by Lowry assay) for BceR-P. The quite low percentage of “active” protein compared to total protein does not necessarily mean that most of the protein is inactive due to misfolding and/or aggregation. It

is rather possible that not the complete amount is phosphorylated and therefore not "active" and/or that, although thoroughly washed with high salts, a portion of the protein has still DNA bound after the purification process. However, the „active" protein concentration was ultimately used for calculation of the binding kinetic constants.

Interaction map® (IM) analyses

IM calculations were performed on the Ridgeview Diagnostic Server (Ridgeview Diagnostics, Uppsala, Sweden). For this purpose, the SPR sensorgrams were exported from the Biacore T200 Evaluation Software 2.0 as *.txt files and imported into TraceDrawer Software 1.5 (Ridgeview Instruments, Uppsala, Sweden). IM files were generated using the IM tool within the software, which produces files that were then sent via e-mail to the server (im@ridgeviewdiagnostics.com), where the IM calculations were performed (Altschuk *et al.* 2012). The resulting files were then evaluated for spots in the TraceDrawer 1.5 Software, and the IM spots were quantified.

Acknowledgements

The authors would like to thank Ainhoa Revilla Guarinos for critical reading of the manuscript and Julia Frunzke for the gift of synthetic phosphoramidate. This work was supported by a grant from the Deutsche Forschungsgemeinschaft (DFG; grant MA2837/1-3 to TM, and Exc114/2 to KJ). CF was supported by a PhD scholarship from the China Scholarship Council. SPR experiments were performed in the Bioanalytics core facility of the LMU Biocenter.

References

Altschuh D., Björkelund, H., Strandgård, J., Choulier, L., Malmqvist, M., and Andersson, K. (2012) Deciphering complex protein interaction kinetics using Interaction Map. *Biochem Biophys Res Commun* **428**:74-9.

Arnaud, M., Chastanet, A., and Débarbouillé, M. (2004) New vector for efficient allelic replacement in naturally nontransformable, low-GC-content, gram-positive bacteria. *Appl Environ Microbiol* **70**: 6887-6891.

Behr, S., Heermann, R., and Jung, K. (2016) Insights into the DNA-binding mechanism of a LytTR-type transcripton regulator. *Biosci Rep* **36**: e00326.

Berdy, J. (2005) Bioactive microbial metabolites. *J Antibiot (Tokyo)* **58**: 1-26.

Bernard, R., Guiseppi, A., Chippaux, M., Foglino, M., and Denizot, F. (2007) Resistance to bacitracin in *Bacillus subtilis*: unexpected requirement of the BceAB ABC transporter in the control of expression of its own structural genes. *J Bacteriol* **189**: 8636-8642.

Blanco, A.G., Canals, A., Bernués, J., Solà, M., and Coll, M. (2011) The structure of a transcription activation subcomplex reveals how sigma70 is recruited to PhoB promoters. *EMBO J* **30**: 3776-3785.

Blanco, A.G., Canals, A., and Coll, M. (2012) PhoB transcriptional activator binds hierarchically to pho box promoters. *Biol Chem* **393**: 1165-1171.

Blanco, A.G., Solà, M., Gomis-Rüth, F.X. and Coll, M. (2002) Tandem DNA recognition by PhoB, a two-component signal transduction transcriptional activator. *Structure* **10**: 701-713.

Bourret, R.B. (2010) Receiver domain structure and function in response regulator proteins. *Curr Opin Microbiol* **13**: 142-149.

Breukink, E., and de Kruijff, B. (2006) Lipid II as a target for antibiotics. *Nat Rev Drug Discov* **5**: 321-323.

Buescher, J.M., Liebermeister, W., Jules, M., Uhr, M., Muntel, J., Botella, E., et al. (2012) Global network reorganization during dynamic adaptations of *Bacillus subtilis* metabolism. *Science* **335**: 1099-1103.

de Been, M., Bart, M.J., Abee, T., Siezen, R.J., and Francke, C. (2008) The identification of response regulator-specific binding sites reveals new roles of two-component systems in *Bacillus cereus* and closely related low-GC Gram-positives. *Environ Microbiol* **10**: 2796-2809.

Dintner, S., Heermann, R., Fang, C., Jung, K., and Gebhard, S. (2014) A sensory complex consisting of an ATP-binding cassette transporter and a two-component regulatory system controls bacitracin resistance in *Bacillus subtilis*. *J Biol Chem* **289**: 27899-27910.

Dintner, S., Staroń, A., Berchtold, E., Petri, T., Mascher, T., and Gebhard, S. (2011) Coevolution of ABC transporters and two-component regulatory systems as resistance modules against antimicrobial peptides in Firmicutes bacteria. *J Bacteriol* **193**: 3851-3862.

Fabret, C., Feher, V.A., and Hoch, J.A. (1999) Two-component signal transduction in *Bacillus subtilis*: how one organism sees its world. *J Bacteriol* **181**: 1975-1983.

Friedlander, T., Prizak, R., Guet, C.C., Barton, N.H., and Tkacik, G. (2016) Intrinsic limits to gene regulation by global crosstalk. *Nat Commun* **7**: 12307.

Fritz, G., Dintner, S., Treichel, N.S., Radeck, J., Gerland, U., Mascher, T., and Gebhard, S. (2015) A new way of sensing: need-based activation of antibiotic resistance by a flux-sensing mechanism. *mBio* **6**: e00975-00915.

Galperin, M.Y. (2006) Structural classification of bacterial response regulators: diversity of output domains and domain combinations. *J Bacteriol* **188**: 4169-4182.

Galperin, M.Y. (2010) Diversity of structure and function of response regulator output domains. *Curr Opin Microbiol* **13**: 150-159.

Gao, R., and Stock, A.M. (2009) Biological insights from structures of two-component proteins. *Annu Rev Microbiol* **63**: 133-154.

Gebhard, S., and Mascher, T. (2011) Antimicrobial peptide sensing and detoxification modules: unravelling the regulatory circuitry of *Staphylococcus aureus*. *Mol Microbiol* **81**: 581-587.

Grant, S.G., Jessee, J., Bloom, F.R., and Hanahan, D. (1990) Differential plasmid rescue from transgenic mouse DNAs into *Escherichia coli* methylation-restriction mutants. *Proc Natl Acad Sci* **87**: 4645-4649.

Harlocker, S.L., Bergstrom, L., and Inouye, M. (1995) Tandem binding of six OmpR proteins to the ompF upstream regulatory sequence of *Escherichia coli*. *J Biol Chem* **270**: 26849-26856.

Harwood, C.R., and Cutting, S.M. (1990) *Molecular biological methods for Bacillus*. Chichester: John Wiley and Sons.

Huynh, T.N., and Stewart, V. (2011) Negative control in two-component signal transduction by transmitter phosphatase activity. *Mol Microbiol* **82**: 275-286.

Jarmer, H., Larsen, T.S., Krogh, A., Saxild, H.H., Brunak, S., and Knudsen, S. (2001) Sigma A recognition sites in the *Bacillus subtilis* genome. *Microbiology* **147**: 2417-2424.

Jordan, S., Hutchings, M.I., and Mascher, T. (2008) Cell envelope stress response in Gram-positive bacteria. *FEMS Microbiol Rev* **32**: 107-146.

Joseph, P., Fichant, G., Quentin, Y., and Denizot, F. (2002) Regulatory relationship of two-component and ABC transport systems and clustering of their genes in the *Bacillus/Clostridium* group, suggest a functional link between them. *J Mol Microbiol Biotechnol* **4**: 503-513.

Koo, H.-S., Wu, H.-M., and Crothers, D.M. (1986) DNA bending at adenine-thymine tracts. *Nature* **320**: 501-506.

Kumar, A., B. Grimes, N. Fujita, K. Makino, R.A. Malloch, R.S. Hayward & A. Ishihama, (1994) Role of the sigma 70 subunit of Escherichia coli RNA polymerase in transcription activation. *Journal of molecular biology* **235**: 405-413.

Lee, D.J., Minchin, S.D., and Busby, S.J.W. (2012) Activating transcription in bacteria. *Annu Rev Microbiol* **66**: 125-152.

Martínez-Hackert, E., and Stock, A.M. (1997) The DNA-binding domain of OmpR: crystal structures of a winged helix transcription factor. *Structure* **5**: 109-124.

Mascher, T., Margulis, N.G., Wang, T., Ye, R.W., and Helmann, J.D. (2003) Cell wall stress responses in *Bacillus subtilis*: the regulatory network of the bacitracin stimulon. *Mol Microbiol* **50**: 1591-1604.

Mascher, T., Zimmer, S.L., Smith, T.A., and Helmann, J.D. (2004) Antibiotic-inducible promoter regulated by the cell envelope stress-sensing two-component system LiaRS of *Bacillus subtilis*. *Antimicrob Agents Chemother* **48**: 2888-2896.

Miller, J.H. (1972) *Experiments in molecular genetics*. Cold Spring Harbor, New York: Cold Spring Harbor Laboratory Press.

Miroux, B., and Walker, J.E. (1996) Over-production of proteins in *Escherichia coli*-mutant hosts that allow synthesis of some membrane proteins and globular proteins at high Levels. *J Mol Biol* **260**: 289-298.

Ohki, R., Giyanto, Tateno, K., Masuyama, W., Moriya, S., Kobayashi, K., and Ogasawara, N. (2003) The BceRS two-component regulatory system induces expression of the bacitracin transporter, BceAB, in *Bacillus subtilis*. *Mol Microbiol* **49**: 1135-1144.

Paget, M., and Helmann, J.D. (2003) The sigma70 family of sigma factors. *Genome Biol* **4**: 203.

Podgornaia, A.I., and Laub, M.T. (2013) Determinants of specificity in two-component signal transduction. *Curr Opin Microbiol* **16**: 156-162.

Procaccini, A., Lunt, B., Szurmant, H., Hwa, T., and Weigt, M. (2011) Dissecting the specificity of protein-protein interaction in bacterial two-component signaling: orphans and crosstalks. *PLoS ONE* **6**: e19729.

Rietkötter, E., Hoyer, D., and Mascher, T. (2008) Bacitracin sensing in *Bacillus subtilis*. *Mol Microbiol* **68**: 768-785.

Silver, L.L. (2003) Novel inhibitors of bacterial cell wall synthesis. *Curr Opin Microbiol* **6**: 431-438.

Staroń, A., Finkeisen, D.E., and Mascher, T. (2011) Peptide antibiotic sensing and detoxification modules of *Bacillus subtilis*. *Antimicrob Agents Chemother* **55**: 515-525.

Stülke, J., Martin-Verstraete, I., Zagorec, M., Rose, M., Klier, A., and Rapoport, G. (1997) Induction of the *Bacillus subtilis ptsGHI* operon by glucose is controlled by the novel antiterminator, GlcT. *Mol microbiol* **25**: 65-78.

Tables

Table S1. Bacterial strains used in this study.

Strain	Genotype or characteristic(s)[a]	Reference or source
E. coli strains		
DH5α	*rec*A1 *end*A1 *gyr*A96 *thi*-1 *hsd*R17 (r_K^- m_K^+) *rel*A1 *gln*V44 *Φ80'* Δ*lacZ* Δ*M15* Δ*(lacZYA-argF)U169*	(Grant *et al.*, 1990)
XL1-Blue	*end*A1 *gyr*A96 *(nal^R) thi*-1 *rec*A1 *rel*A1 *lac sup*E44 [F' *pro*AB$^+$ *lacI*^{q} *Δ(lacZ)M15] hsd*R17(r_K^- m_K^+)	Stratagene
C43 (DE3)	F$^-$ *omp*T *gal dcm hsdS$_B$* (r_B^- m_B^-)(DE3)	(Miroux & Walker, 1996)
B. subtilis strains		
W168	Wild type, *trpC2*	Laboratory stock
TMB279	W168 *amyE*::pER603; cm^r	(Rietkötter *et al.*, 2008)
TMB299	W168 *amyE*::pER605; cm^r	(Rietkötter *et al.*, 2008)
TMB412	W168 *amyE*::pCF601; cm^r	This study
TMB607	W168 *amyE*::pJS605; cm^r	This study
TMB805	W168 *amyE*::pAS601; cm^r	This study
TMB806	W168 *amyE*::pAS602; cm^r	This study
TMB960	W168 *amyE*::pAS603; cm^r	This study
TMB961	W168 *amyE*::pAS604; cm^r	This study
TMB962	W168 *amyE*::pAS605; cm^r	This study
TMB963	W168 *amyE*::pAS606; cm^r	This study
TMB964	W168 *amyE*::pAS607; cm^r	This study
TMB965	W168 *amyE*::pAS608; cm^r	This study
TMB966	W168 *amyE*::pAS609; cm^r	This study
TMB967	W168 *amyE*::pAS610; cm^r	This study
TMB1047	W168 *amyE*::pAS613; cm^r	This study
TMB1048	W168 *amyE*::pAS614; cm^r	This study
TMB1049	W168 *amyE*::pAS615; cm^r	This study
TMB1050	W168 *amyE*::pAS616; cm^r	This study
TMB1051	W168 *amyE*::pAS617; cm^r	This study
TMB1052	W168 *amyE*::pAS618; cm^r	This study
TMB1053	W168 *amyE*::pAS619; cm^r	This study
TMB1054	W168 *amyE*::pAS620; cm^r	This study
TMB1460	W168 with unmarked deletions of the *bceRS* loci	This study
TMB1462	W168 with unmarked deletions of the *psdRS* loci	This study
TMB2244	W168 *amyE*::pMG600; cm^r	This study
TMB2245	W168 *amyE*::pMG601; cm^r	This study
TMB2247	W168 *amyE*::pMG603; cm^r	This study
TMB2248	W168 *amyE*::pMG604; cm^r	This study
TMB2249	W168 *amyE*::pMG605; cm^r	This study
TMB2250	W168 *amyE*::pMG606; cm^r	This study
TMB2252	W168 *amyE*::pMG608; cm^r	This study
TMB2253	W168 *amyE*::pMG609; cm^r	This study
TMB2303	TMB1462 *amyE*::pER603; cm^r	This study
TMB2304	TMB1462 *amyE*::pCF601; cm^r	This study
TMB2307	TMB1460 *amyE*::pER603; cm^r	This study
TMB2308	TMB1460 *amyE*::pCF601; cm^r	This study
TMB2382	TMB1460 *amyE*::pMG600; cm^r	This study
TMB2383	TMB1460 *amyE*::pMG601; cm^r	This study
TMB2385	TMB1460 *amyE*::pMG603; cm^r	This study
TMB2386	TMB1460 *amyE*::pMG604; cm^r	This study
TMB2387	TMB1462 *amyE*::pMG600; cm^r	This study

TMB2388	TMB1462 *amyE*::pMG601; cm^r	This study
TMB2390	TMB1462 *amyE*::pMG603; cm^r	This study
TMB2391	TMB1462 *amyE*::pMG604; cm^r	This study
TMB2392	TMB1460 *amyE*::pMG605; cm^r	This study
TMB2393	TMB1460 *amyE*::pMG606; cm^r	This study
TMB2395	TMB1460 *amyE*::pMG608; cm^r	This study
TMB2396	TMB1460 *amyE*::pMG609; cm^r	This study
TMB2397	TMB1462 *amyE*::pMG606; cm^r	This study
TMB2399	TMB1462 *amyE*::pMG608; cm^r	This study
TMB2400	TMB1462 *amyE*::pMG609; cm^r	This study
TMB2455	W168 *amyE*::pMG612; cm^r	This study
TMB2456	W168 *amyE*::pMG613; cm^r	This study
TMB2457	W168 *amyE*::pMG614; cm^r	This study
TMB2460	W168 *amyE*::pMG617; cm^r	This study
TMB2461	W168 *amyE*::pMG618; cm^r	This study
TMB2462	W168 *amyE*::pMG619; cm^r	This study
TMB2463	TMB1462 *amyE*::pMG614; cm^r	This study
TMB2464	TMB1460 *amyE*::pMG614; cm^r	This study
TMB2465	TMB1462 *amyE*::pMG613; cm^r	This study
TMB2466	TMB1460 *amyE*::pMG613; cm^r	This study
TMB2467	TMB1462 *amyE*::pMG619; cm^r	This study
TMB2468	TMB1460 *amyE*::pMG619; cm^r	This study
TMB2469	TMB1462 *amyE*::pMG618; cm^r	This study
TMB2470	TMB1460 *amyE*::pMG618; cm^r	This study
TMB2475	TMB1462 *amyE*::pMG605; cm^r	This study
TMB2505	W168 *amyE*::pCF608; cm^r	This study
TMB2506	W168 *amyE*::pCF609; cm^r	This study
TMB2507	W168 *amyE*::pCF610; cm^r	This study
TMB2508	W168 *amyE*::pCF611; cm^r	This study
TMB2509	W168 *amyE*::pMG621; cm^r	This study
TMB2510	TMB1460 *amyE*::pMG621; cm^r	This study
TMB2511	TMB1462 *amyE*::pMG621; cm^r	This study
TMB2512	W168 *amyE*::pMG622; cm^r	This study
TMB2513	TMB1460 *amyE*::pMG622; cm^r	This study
TMB2514	TMB1462 *amyE*::pMG622; cm^r	This study
TMB2515	W168 *amyE*::pCF612; cm^r	This study
TMB2516	TMB1460 *amyE*::pCF612; cm^r	This study
TMB2517	TMB1462 *amyE*::pCF612; cm^r	This study
TMB2518	W168 *amyE*::pCF613; cm^r	This study
TMB2519	TMB1460 *amyE*::pCF613; cm^r	This study
TMB2520	TMB1462 *amyE*::pCF613; cm^r	This study
TMB2536	W168 *amyE*::pCF614; cm^r	This study
TMB2537	TMB1460 *amyE*::pCF614; cm^r	This study
TMB2538	TMB1462 *amyE*::pCF614; cm^r	This study
TMB2539	W168 *amyE*::pCF615; cm^r	This study
TMB2540	TMB1460 *amyE*::pCF615; cm^r	This study
TMB2541	TMB1462 *amyE*::pCF615; cm^r	This study
TMB2631	W168 *amyE*::pCF616	This study
TMB2632	TMB1460 *amyE*::pCF616	This study
TMB2633	TMB1462 *amyE*::pCF616	This study
TMB2637	W168 *amyE*::pCF618	This study
TMB2638	TMB1460 *amyE*::pCF618	This study
TMB2639	TMB1462 *amyE*::pCF618	This study
TMB2640	W168 *amyE*::pCF619; cm^r	This study
TMB2641	TMB1460 *amyE*::pCF619; cm^r	This study
TMB2642	TMB1462 *amyE*::pCF619; cm^r	This study
TMB2643	W168 *amyE*::pCF620; cm^r	This study
TMB2644	TMB1460 *amyE*::pCF620; cm^r	This study
TMB2645	TMB1462 *amyE*::pCF620; cm^r	This study

[a] Resistant cassettes: cm, chloramphenicol; r, resistant.

819 **Table S2.** Vectors and plasmids used in this study.

Plasimd	Genotype or characteristic(s)	Primers used for cloning	Reference or source
Vectors			
pAC6	Vector for transcriptional promoter fusions to *lacZ* in *B. subtilis*, integrates in *amyE*; cm^r		(Stülke *et al.*, 1997)
pET16b	Vector for IPTG-inducible gene expression; carries a N-terminal His_{10}-tag sequence; amp^r		Novagen
pMAD	Vector for construction of unmarked deletions in *B. subtilis*, temperature sensitive replicon; mls^r		(Arnaud *et al.*, 2004)
Plasmids			
pAS601	pAC6 P_{psdA} (-99 to +30) -*lacZ*	1591/0600	This study
pAS602	pAC6 P_{psdA} (-97 to +30) -*lacZ*	1592/0600	This study
pAS603	pAC6 P_{psdA} (-104 to +30) -*lacZ*	1688/0600	This study
pAS604	pAC6 P_{psdA} (-103 to +30) -*lacZ*	1687/0600	This study
pAS605	pAC6 P_{psdA} (-102 to +30) -*lacZ*	1686/0600	This study
pAS606	pAC6 P_{psdA} (-101 to +30) -*lacZ*	1685/0600	This study
pAS607	pAC6 P_{psdA} (-100 to +30) -*lacZ*	1684/0600	This study
pAS608	pAC6 P_{psdA} (-98 to +30) -*lacZ*	1683/0600	This study
pAS609	pAC6 P_{psdA} (-96 to +30) -*lacZ*	1682/0600	This study
pAS610	pAC6 P_{psdA} (-95 to +30) -*lacZ*	1681/0600	This study
pAS613	pAC6 P_{bceA} (-110 to +82) -*lacZ*	1869/0555	This study
pAS614	pAC6 P_{bceA} (-109 to +82) -*lacZ*	1870/0555	This study
pAS615	pAC6 P_{bceA} (-108 to +82) -*lacZ*	1871/0555	This study
pAS616	pAC6 P_{bceA} (-107 to +82) -*lacZ*	1872/0555	This study
pAS617	pAC6 P_{bceA} (-106 to +82) -*lacZ*	1873/0555	This study
pAS618	pAC6 P_{bceA} (-105 to +82) -*lacZ*	1874/0555	This study
pAS619	pAC6 P_{bceA} (-104 to +82) -*lacZ*	1875/0555	This study
pAS620	pAC6 P_{bceA} (-103 to +82) -*lacZ*	1876/0555	This study
pCF101	pMAD Δ*bceRS*	2351/2352 2353/2354	This study
pCF103	pMAD Δ*psdRS*	2357/2358 2359/2360	This study
pCF120	pET16b *bceR*	2007/2008	This study
pCF601	pAC6 P_{psdA} (-126 to +30)-*lacZ*	0674/0600	This study
pCF608	pAC6 P_{bceA} (-122 to +82) main binding site mutation-*lacZ*	2262/3563 3564/0555	This study
pCF609	pAC6 P_{bceA} (-122 to +82) second binding site mutation-*lacZ*	0554/3565 3566/0555	This study
pCF610	pAC6 P_{psdA} (-126 to +30) main binding site mutation-*lacZ*	2262/3567 3568/0600	This study
pCF611	pAC6 P_{psdA} (-126 to +30) second binding site mutation-*lacZ*	0674/3569 3570/0600	This study
pCF612	pAC6 P_{psdA} (-126 to +30) second binding site switched into the corresponding region of P_{bceA} -*lacZ*	0674/3553 3554/0600	This study
pCF613	pAC6 P_{psdA} (-126 to +30) linker and second binding site switched into the corresponding region of P_{bceA} -*lacZ*	0674/3557 3558/0600	This study
pCF614	pAC6 P_{bceA} (-122 to +82) main binding site, linker and second binding site switched into the corresponding region of P_{psdA} -*lacZ*	3692/0555	This study
pCF615	pAC6 P_{psdA} (-126 to +30) main binding site, linker and second binding site switched into the corresponding region of P_{bceA} -*lacZ*	3693/0600	This study
pCF616	pAC6 P_{bceA} (-122 to +82) main binding site and second binding site switched into the corresponding region of P_{psdA} -*lacZ*	3719/0555	This study

pCF618	pAC6 P_{bceA} (-122 to +82) main binding site and linker switched into the corresponding region of P_{psdA} -*lacZ*	3721/0555	This study
pCF619	pAC6 P_{psdA} (-126 to +30) main binding site and second binding site switched into the corresponding region of P_{bceA} -*lacZ*	3720/0600	This study
pCF620	pAC6 P_{psdA} (-126 to +30) main binding site and linker switched into the corresponding region of P_{bceA} -*lacZ*	3722/0600	This study
pER603	pAC6 P_{bceA} (-122 to +82) -*lacZ*	0554/0555	(Rietkötter *et al.*, 2008)
pER605	pAC6 P_{psdA} (-110 to +30)-*lacZ*	0599/0600	(Rietkötter *et al.*, 2008)
pMG600	pAC6 P_{bceA} (-122 to -46) - P_{psdA} (-36 to +30) (BP1) -*lacZ*	1689/3240 3241/0600	This study
pMG601	pAC6 P_{bceA} (-122 to -56) - P_{psdA} (-46 to +30) (BP2) -*lacZ*	1689/3242 3243/0600	This study
pMG603	pAC6 P_{bceA} (-122 to -76) - P_{psdA} (-66 to +30) (BP3) -*lacZ*	1689/3246 3247/0600	This study
pMG604	pAC6 P_{bceA} (-122 to -88) - P_{psdA} (-79 to +30) (BP4) -*lacZ*	1689/3248 3249/0600	This study
pMG605	pAC6 P_{psdA} (-126 to -37) - P_{bceA} (-45 to +82) (PB1) -*lacZ*	0674/3230 3231/0555	This study
pMG606	pAC6 P_{psdA} (-126 to -47) - P_{bceA} (-55 to +82) (PB2) -*lacZ*	0674/3232 3233/0555	This study
pMG608	pAC6 P_{psdA} (-126 to -67) - P_{bceA} (-75 to +82) (PB3) -*lacZ*	0674/3236 3237/0555	This study
pMG609	pAC6 P_{psdA} (-126 to -80) - P_{bceA} (-87 to +82) (PB4) -*lacZ*	0674/3238 3239/0555	This study
pMG612	pAC6 P_{bceA} (-122 to + 82) linker mutation -*lacZ*	0146/3351 3395/0010	This study
pMG613	pAC6 P_{bceA} (-122 to + 82) linker switched into the corresponding part of P_{psdA} -*lacZ*	0146/3401 3400/0010	This study
pMG614	pAC6 P_{bceA} (-122 to + 82) main binding site switched into the corresponding region of P_{psdA} -*lacZ*	0146/3419 3354/0010	This study
pMG617	pAC6 P_{psdA} (-126 to + 30) linker mutation -*lacZ*	0146/3353 3352/0600	This study
pMG618	pAC6 P_{psdA} (-126 to + 30) linker switched into the corresponding region of P_{bceA} -*lacZ*	0146/3403 3402/0600	This study
pMG619	pAC6 P_{psdA} (-126 to + 30) main binding site switched into the corresponding region of P_{bceA} -*lacZ*	0146/3357 3356/0600	This study
pMG621	pAC6 P_{bceA} (-122 to + 82) second binding site switched into the corresponding region of P_{psdA} -*lacZ*	2262/3551 3552/0555	This study
pMG622	pAC6 P_{bceA} (-122 to + 82) linker and the second binding site switched into the corresponding region of P_{psdA} -*lacZ*	2262/3555 3556/0555	This study
pJS605	pAC6 P_{bceA} (-111 to +82) -*lacZ*	1307/0555	This study

Amp, ampicillin; cm, chloramphenicol; mls, macrolide-lincosamide-streptogramin B group antibiotics; r, resistant.

Supplemental Table S3. Primers used in this study.

Primer name	Sequence (5'-3')[a]	Use
TM0010	CTTCGCTATTACGCCAGCTGG	*lacZ* check rev
TM0146	GTCTGCTTTCTTCATTAGAATCAATCC	*cat* check rev
TM0554	GATCGAATTCGAACATGTCATAAGCGTGTGACG	P_{bceA} (-122) fwd
TM0555	GATCGGATCCTATCGATGCCCTTCAGCACTTCC	P_{bceA} rev
TM0599	AGTCGAATTCCACCCTCGTGAATGTGACAGC	P_{psdA} (-110) *fwd*
TM0600	AGTCGGATCCCGATAGGTTCGTTGTTTGCAACACG	P_{psdA} rev
TM0674	AGTCGAATTCTCGTGTTTTCAAGTGACACC	P_{psdA} (-126) fwd
TM1307	GATCGAATTCAAGCGTGTGACGAAAATGTCACAT	P_{bceA} (-111) fwd
TM1591	AGTCGAATTCATGTGACAGCATTGTAAGATTGG	P_{psdA} (-99) fwd
TM1592	AGTCGAATTCGTGACAGCATTGTAAGATTGG	P_{psdA} (-97) fwd
TM1681	AGTCGAATTCACGACAGCATTGTAAGATTGG	P_{psdA} (-95) fwd
TM1682	AGTCGAATTCATGACAGCATTGTAAGATTGG	P_{psdA} (-96) fwd
TM1683	AGTCGAATTCTGTGACAGCATTGTAAGATTGG	P_{psdA} (-98) fwd
TM1684	AGTCGAATTCTAATGTGACAGCATTGTAAG	P_{psdA} (-100) fwd
TM1685	AGTCGAATTCGAATGTGACAGCATTGTAAG	P_{psdA} (-101) fwd
TM1686	AGTCGAATTCTGAATGTGACAGCATTGTAAG	P_{psdA} (-102) fwd
TM1687	AGTCGAATTCAGTGAATGTGACAGCATTGTAAG	P_{psdA} (-103) fwd
TM1688	AGTCGAATTCCGTGAATGTGACAGCATTGTAAG	P_{psdA} (-104) fwd
TM1689	CCGATGATAAGCTGTCAAAC	pAC6 bandshifts
TM1869	ATGCGAATTCAGCGTGTGACGAAAATG	P_{bceA} (-110) fwd
TM1870	ATGCGAATTCGCGTGTGACGAAAATGTC	P_{bceA} (-109) fwd
TM1871	ATGCGAATTCACGTGTGACGAAAATGTC	P_{bceA} (-108) fwd
TM1872	ATGCGAATTCAAGTGTGACGAAAATGTC	P_{bceA} (-107) fwd
TM1873	ATGCGAATTCAAATGTGACGAAAATGTC	P_{bceA} (-106) fwd
TM1874	ATGCGAATTCGTGACGAAAATGTCAC	P_{bceA} (-105) fwd
TM1875	ATGCGAATTCATGACGAAAATGTCAC	P_{bceA} (-104) fwd
TM1876	ATGCGAATTCAAGACGAAAATGTCAC	P_{bceA} (-103) fwd
TM2007	ATCGCTCGAGTTGTTTAAACTTTTGCTGATTG	*bceR* fwd
TM2008	ATCGGGATCCTTAATCATAGAACTTGTCCTC	*bceR* rev
TM2262	GAGCGTAGCGAAAAATCC	pAH328 checkfwd
TM2351	AATTTGGATCCGAGGAAGCAAAAGGAAATC	*bceRS* deletion up fwd
TM2352	CTTGATTTCATGAAACAGCG	*bceRS* deletion up rev
TM2353	ctgtttcatgaaatcaag ATATTGATGTTGAGTCGGAG	*bceRS* deletion down fwd
TM2354	AATTCCATGGTTCAAATTTCGCAGGATGAG	*bceRS* deletion down rev
TM2357	AATTTGGATCCCTACGATCTAAATGGTTTCC	*psdRS* deletion up fwd
TM2358	ATTTTTGAAGATGACCGCCC	*psdRS* deletion up rev
TM2359	cggtcatcttcaaaaat CACTGTGATGACCATCGTG	*psdRS* deletion down fwd
TM2360	AATTCCATGGACCGAAACGGCAAACACAC	*psdRS* deletion down rev
TM3230	GTCAGCATCCTCCCATCGAAC	PB1 up rev
TM3231	cgatgggaggatgctgac TTCCTTTTTATAATGAGATTATCC	PB1 down fwd
TM3232	TCCCATCGAACTTTCTTGCAATTC	PB2 up rev
TM3233	caagaaagttcgatggga AAGCCCGGCATTCCTTTTTATAATG	PB2 down fwd
TM3236	TTCCGCTCCCCAATCTTACAATG	PB3 up rev
TM3237	taagattggggagcggaa TTGTTCGCCGTATCGAAGG	PB3 down fwd
TM3238	ATCTTACAATGCTGTCACATTC	PB4 up rev
TM3239	gtgacagcattgtaagat GCTTTTCTTTTTTGTTCGCCG	PB4 down fwd
TM3240	TGCCGGGCTTTTCCTTCGATAC	BP1 up rev
TM3241	cgaaggaaaagcccggcaTTCCTTTTTATAATAAAGAAAAAGG	BP1 down fwd
TM3242	TTCCTTCGATACGGCGAAC	BP2 up rev
TM3243	ttcgccgtatcgaaggaaGGATGCTGACTTCCTTTTTATAATAAAG	BP2 down fwd
TM3246	AAAAGAAAAGCATGTGACATTTTC	BP3 up rev
TM3247	gtcacatgcttttctttTTGCAAGAAAGTTCGATGGGAGG	BP3 down fwd
TM3248	ATGTGACATTTTCGTCACACGC	BP4 up rev
TM3249	gtgacgaaaatgtcacatTGGGGAGCGGAATTGCAAGAAAG	BP4 down fwd
TM3351	cgaacaaatttgtataGCATGTGACATTTTCGTC	P_{bceA} L-M up rev
TM3352	cgcacggcaattgcaAGAAAGTTCGATGGGAGG	P_{psdA} L-M down fwd
TM3353	tgcaattgccgtgcgCAATCTTACAATGCTGTCAC	P_{psdA} L-M up rev
TM3354	gacagcattgtaagaTGCTTTTCTTTTTTGTTCGCC	P_{bceA} M-S down fwd
TM3356	gacgaaaatgtcacaTTGGGGAGCGGAATTGCAAG	P_{psdA} M-S down fwd
TM3357	tgtgacattttcgtcACATTCACGAGGGTGTCACTTG	P_{psdA} M-S up rev
TM3395	tatacaaatttgttcgCCGTATCGAAGGAAAAGC	P_{bceA} L-M down fwd
TM3400	ggcgaacaatccgctcccGCATGTGACATTTTCGTCAC	P_{bceA} L-S down fwd

TM3401	gggagcggattgttcgccGTATCGAAGG	P_{bceA} L-S up rev
TM3402	cttgcaataaaagaaaaCAATCTTACAATGCTGTCAC	P_{psdA} L-S down fwd
TM3403	ttttcttttattgcaagAAAGTTCGATGGG	P_{psdA} L-S up rev
TM3419	tcttacaatgctgtcACACGCTTATGACATGTTCG	P_{bceA} M-S up rev
TM3551	ccatcgaactttcttgCAAAAAAGAAAAGCATGTGACATTTTC	P_{bceA} S-S up rev
TM3552	caagaaagttcgatGGAAAAGCCCGGCATTCC	P_{bceA} S-S down fwd
TM3553	ccttcgatacggcgaaCAATTCCGCTCCCCAATC	P_{psdA} S-S up rev
TM3554	ttcgccgtatcgaaGGGAGGATGCTGACTTCC	P_{psdA} S-S down fwd
TM3555	actttcttgcaattccgctccccaATGTGACATTTTCGTCACACG	P_{bceA} S+L-S up rev
TM3556	ggaattgcaagaaagttcgatGGAAAAGCCCGGCATTCC	P_{bceA} S+L-S down fwd
TM3557	tacggcgaacaaaaaagaaaagcATCTTACAATGCTGTCACATTC	P_{psdA} S+L-S up rev
TM3558	ttttttgttcgccgtatcgaaGGGAGGATGCTGACTTCC	P_{psdA} S+L-S down fwd
TM3563	gcgttaagtcaccgctaaCGCTTATGACATGTTCGAATTCG	P_{bceA} M-M up rev
TM3564	ttagcggtgacttaacgcTGCTTTTCTTTTTTGTTCGCCG	P_{bceA} M-M down fwd
TM3565	cagctagcagtcagtcagAAAAAGAAAAGCATGTGACATTTTC	P_{bceA} S-M up rev
TM3566	ctgactgactgctagctgAAAAGCCCGGCATTCCTTTT	P_{bceA} S-M down fwd
TM3567	tacttcggtcaccgctaaTTCACGAGGGTGTCACTTG	P_{psdA} M-M up rev
TM3568	ttagcggtgaccgaagtaTTGGGGAGCGGAATTGCAAG	P_{psdA} M-M down fwd
TM3569	gtcagtcgtcagtcagtcATTCCGCTCCCCAATCTTAC	P_{psdA} S-M up rev
TM3570	gactgactgacgactgacGAGGATGCTGACTTCCTTTT	P_{psdA} S-M down fwd
TM3665	GTCATAAGCGTGTGACGAAAATGTCACATGCTTTTCTTTTTTGTTC GCCGTATCGAAGGAAAAGCCCGGCATTCCT	P_{bceA} WT fwd (for SPR)
TM3666	AGGAATGCCGGGCTTTTCCTTCGATACGGCGAACAAAAAAGAAA AGCATGTGACATTTTCGTCACACGCTTATGAC	Biotin-P_{bceA} WT rev (for SPR)
TM3667	CCCTCGTGAATGTGACAGCATTGTAAGATTGGGGAGCGGAATTG CAAGAAAGTTCGATGGGAGGATGCTGACTTCCT	P_{psdA} WT fwd (for SPR)
TM3668	AGGAAGTCAGCATCCTCCCATCGAACTTTCTTGCAATTCCGCTCC CCAATCTTACAATGCTGTCACATTCACGAGGG	Biotin-P_{psdA} WT rev (for SPR)
TM3669	GTCATAAGCGTTAGCGGTGACTTAACGCTGCTTTTCTTTTTTGTTC GCCGTATCGAAGGAAAAGCCCGGCATTCCT	P_{bceA} M-M fwd (for SPR)
TM3670	AGGAATGCCGGGCTTTTCCTTCGATACGGCGAACAAAAAAGAAA AGCAGCGTTAAGTCACCGCTAACGCTTATGAC	Biotin-P_{bceA} M-M rev (for SPR)
TM3671	CCCTCGTGAATTAGCGGTGACCGAAGTATTGGGGAGCGGAATTG CAAGAAAGTTCGATGGGAGGATGCTGACTTCCT	P_{psdA} M-M fwd (for SPR)
TM3672	AGGAAGTCAGCATCCTCCCATCGAACTTTCTTGCAATTCCGCTCC CCAATACTTCGGTCACCGCTAATTCACGAGGG	Biotin-P_{psdA} M-M rev (for SPR)
TM3673	GTCATAAGCGTGTGACGAAAATGTCACATGCTTTTCTTTTTCTGA CTGACTGCTAGCTGAAAAGCCCGGCATTCCT	P_{bceA} S-M fwd (for SPR)
TM3674	AGGAATGCCGGGCTTTTCAGCTAGCAGTCAGTCAGAAAAAGAAA AGCATGTGACATTTTCGTCACACGCTTATGAC	Biotin-P_{bceA} S-M rev (for SPR)
TM3675	CCCTCGTGAATGTGACAGCATTGTAAGATTGGGGAGCGGAATGA CTGACTGACGACTGACGAGGATGCTGACTTCCT	P_{psdA} S-M fwd (for SPR)
TM3676	AGGAAGTCAGCATCCTCGTCAGTCGTCAGTCAGTCATTCCGCTCC CCAATCTTACAATGCTGTCACATTCACGAGGG	Biotin-P_{psdA} S-M rev (for SPR)
TM3677	TCACGAATTACCATCTACACCCTGCCAAAAATTTGATAAACTTAT TTTATAAAAAAATTGAAACCTTTTGAAACGAA	P_{sigW} WT fwd (for SPR)
TM3678	TTCGTTTCAAAAGGTTTCAATTTTTTTATAAAATAAGTTTATCAAA TTTTTGGCAGGGTGTAGATGGTAATTCGTGA	Biotin-P_{sigW} WT rev (for SPR)
TM3692	GATCGAATTCGAACATGTCATAAGCGTGTGACAGCATTGTAAGA TTGGGGAGCGGAATTGC	P_{bceA} M+L+S-S fwd
TM3693	AGTCGAATTCTCGTGTTTTCAAGTGACACCCTCGTGAATGTGACG AAAATGTCACATGCTTTTCTTTTTTGTTCGC	P_{psdA} M+L+S-S fwd
TM3719	GATCGAATTCGAACATGTCATAAGCGTGTGACAGCATTGTAAGA TGCTTTTCTTTTTTGCAAG	P_{bceA} M+S-S fwd
TM3720	AGTCGAATTCTCGTGTTTTCAAGTGACACCCTCGTGAATGTGACG AAAATGTCACATTGGGGAGCGGAATTG	P_{psdA} M+S-S fwd
TM3721	GATCGAATTCGAACATGTCATAAGCGTGTGACAGCATTGTAAGA TTG	P_{bceA} M+L-S fwd
TM3722	AGTCGAATTCTCGTGTTTTCAAGTGACACCCTCGTGAATGTGACG AAAATGTCACATG	P_{psdA} M+L-S fwd

[a] Restriction sites are underlined; overlaps to other primers for PCR fusions are shown by lower case letters.

Figure legends

Figure 1. Model of signal transduction pathways of two Bce-like systems after induction with corresponding AMPs in *Bacillus subtilis*. The TCSs Bce and Psd and their inducing antibiotics as signal inputs are highlighted black and grey, respectively. For reasons of simplicity, the ABC transporters of both systems are not shown. Solid arrows indicate the signal transduction pathway within one system, while cross-regulation between BceS and PsdR is highlighted by the dotted arrow. On each promoter, MBS representing for the main binding site and SBS representing for the secondary binding of Bce-like RRs are filled with white on *bceA* promoter and slashes on *psdA* promoter. CM, cell membrane.

Figure 2. Functional analysis of *bceA* and *psdA* promoters of *B. subtilis*. (A) DNA sequence alignment of the *bceA* promoter and the *psdA* promoter. Different motifs are framed and annotated underneath the DNA sequence. Important positions on each promoter are marked with arrows according to the start codon of the corresponding regulated gene. Half binding sites of Bce-like RRs on each promoter are emphasized in bold face. Activities of (B) truncated constructions of the *bceA* promoter (from -122: +82 to -103: +82) and (C) truncated constructions of the *psdA* promoter (from -126: +30 to -95: +30) according to the start codon of regulated genes. Activities of (D) P_{bceA} mutants and (E) P_{psdA} mutants with MBS^R (main binding site random mutation), L^R (linker random mutation) and SBS^R (secondary binding site random mutation) are compared with the corresponding WT promoters. All promoter constructions were fused to *lacZ* and introduced into *amyE* locus of *B. subtilis* 168. Cultures growing exponentially in LB were challenged with Zn^{2+}-bacitracin 30 μg ml^{-1} (black bars) or nisin 2 μg ml^{-1} (grey bars) for 30 min, comparing with the non-induced condition (white bars). β-galactosidase activities are expressed in Miller Units (MU) (Miller, 1972) and results are

shown as the mean plus standard deviation of three biological replicates. A log scale is applied for reasons of clarity.

Figure 3. Functional studies of chimeric promoters derived from P_{bceA} ("B") and P_{psdA} ("P"). Schematic of series of chimeric promoters (A) BP1-4, *bceA* promoter fragments (black) with gradual substitutions of 3' region by increased corresponding parts of *psdA* promoter (grey) and (B) PB1-4 vice versa are compared with WT P_{bceA} and P_{psdA}. The MBS and SBS of P_{bceA} and P_{psdA} are represented as in Fig.1. Grey dashed lines indicate the fusion points of each chimera. (C to H) Activities of chimeric promoters compared with WT promoters in different genetic backgrounds of *B. subtilis*. Transcriptional *lacZ* fusions of WT promoters (P_{bceA} and P_{psdA}) as well as different sets of chimeras (BP1-4 and PB1-4) were integrated at the *amyE* locus of *B. subtilis* wildtype (WT), Δ*psdRS* strain (TMB1462) and Δ*bceRS* strain (TMB1460). Promoter activities were measured by β-galactosidase assay as described in Fig. 2. (C) BP1-4 in WT, (D) BP1-4 in Δ*psdRS* strain, (E) BP1-4 Δ*bceRS* strain, (F) PB1-4 in WT, (G) PB1-4 in Δ*bceRS* strain and (H) PB1-4 in Δ*psdRS* strain. For reasons of clarity, the values of promoter activities induced by bacitracin are represented as % relative to the native P_{bceA}, while the values of promoter activities induced by nisin are represented as % relative to the native P_{psdA} promoters. Both wild type promoters are set to 100% after subtraction of the uninduced promoter activities. The original data sets corresponding to Fig. 3 are provided in Fig. S1. Black and grey bars, induction with bacitracin and nisin, respectively.

Figure 4. Unravelling the roles of different promoter elements in RR-promoter specificity. (A and B) Schematic of chimeric promoters derived from P_{bceA} and P_{psdA}, respectively. Composition of each chimeric promoter is indicated as follows: M, main binding site; L, linker; S, secondary binding site. MBS and SBS from P_{bceA} and P_{psdA} are indicated as in Fig.1. (C to H) Activities of chimeric promoters compared with WT promoters in different

genetic backgrounds of *B. subtilis*. Transcriptional *lacZ* fusions of WT promoters (P_{bceA} and P_{psdA}) as well as different sets of chimeras from (A) and (B) were integrated at *amyE* locus in *B. subtilis* WT strain, Δ*psdRS* strain (TMB1462) and Δ*bceRS* strain (TMB1460). Promoter activities were measured by β-galactosidase assay as described for Fig. 2. (C) P_{bceA}-derived chimeras in WT, (D) P_{bceA}-derived chimeras in Δ*psdRS* strain, (E) P_{bceA}-derived chimeras in Δ*bceRS* strain, (F) P_{psdA}-derived chimeras in WT, (G) P_{psdA}-derived chimeras in Δ*bceRS* strain and (H) P_{psdA}-derived chimeras in Δ*psdRS* strain. Black bars and grey bars represent samples induced with bacitracin and nisin, respectively. Data representation as described for Fig. 3; original data sets are provided in Fig. S2.

Figure 5. *In vitro* binding of BceR-P to P_{bceA} and P_{psdA}. Increasing concentrations of phosphorylated 10×His-BceR were incubated with 30 fmol of different 6FAM-labeled promoter DNA fragments as follows: (A) P_{bceA} from -122 to +82, (B) P_{psdA} from -126 to +30, (C) P_{bceA} SBS^R (SBS inactivated), (D) P_{bceA} MBS^R (MBS inactivated), and (E) P_{sigW} as a negative control. Schematics of *bceA*-like promoters and corresponding mutants are shown in the lower left corner of each gel. The concentrations of phosphorylated BceR are indicated above the gel by [BceR-P] in μM. 900 fmol of unlabelled competitor (comp.) DNA fragments containing P_{bceA}, P_{psdA} and P_{sigW} were added for lanes 6, 7 and 8, respectively, in (A) and (B).

Figure 6. Surface plasmon resonance spectroscopy of and IM analysis BceR-P binding within the P_{bceA} and P_{psdA} promoter region. (A) BceR binding to P_{bceA}, (B) BceR-P binding to P_{bceA}, (C) BceR-P binding to P_{bceA} MBS^R (MBS inactivated), and (D) BceR-P binding to P_{bceA} SBS^R (SBS inactivated), (E) IM and *in silico* sensorgrams of BceR binding to P_{bceA},; (F) IM and *in silico* sensorgrams of BceR binding to P_{bceA} SBS^R (SBS inactivated), (G) BceR binding to P_{psdA}, (H) BceR-P binding to P_{psdA}, (I) BceR-P binding to P_{psdA} MBS^R, (K) BceR-P binding to P_{psdA} SBS^R), (L) IM and *in silico* sensorgrams of BceR binding to P_{psdA}, and (M)

IM and *in silico* sensorgrams of BceR binding to P_{psdA} SBS^R (SBS inactivated). SPR sensorgrams: 0.2 nM (red line), 0.5 nM (brown line), 1 nM (dark blue line), 2.5 nM (magenta line), 5 nM (green line), 7.5 nM (lime green line), and 10 nM (blue line), respectively, of each of purified BceR or BceR-P was passed over the chip. The sensorgrams show each one representative example of three independently performed experiments. IM analyses: the blue spots in the IMs represent the fast ON/fast OFF interaction, which corresponds to the SBS, the green spots the slow ON/slow OFF interaction corresponding to the higher affine MBS. The respective calculated sensorgrams are shown in the same colors. The calculated overall affinities (K_D), as well as the ON (k_a) and OFF (k_d) rates, are indicated below the respective *in silico* sensorgram. The grey shapes of the IM peaks represent the weighing factors meaning the darker the grey scale, the stronger the contribution.

Figure 7. Model of the specific transcriptional activation of P_{bceA} by BceR and RNA polymerase. Initially, a BceR dimer (black), but not a PsdR dimer (grey) preferentially binds to the MBS of P_{bceA}. This interaction then facilitates the binding of a second BceR dimer to the SBS directly upstream of the -10 element of P_{bceA}. This second binding event then mediates the binding of the σ^A subunit of the RNA polymerase holo-enzyme to the promoter region to ultimately initiate transcription. Presumably, the structure of the DNA is altered by the linker region between two binding sites (DNA bending). See discussion for details.

Figure S1. Functional studies of chimeric promoters derived from P_{bceA} ("B") and P_{psdA} ("P"). Schematic of series of chimeric promoters (A) BP1-4, *bceA* promoter fragments (black) with gradual substitutions of 3' region by increased corresponding parts of *psdA* promoter (grey) and (B) PB1-4 vice versa are compared with WT P_{bceA} and P_{psdA}. The MBS and SBS of P_{bceA} and P_{psdA} are represented as in Fig.1. Grey dashed lines indicate the fusion points of each chimera. (C to H) Activities of chimeric promoters compared with WT promoters in different

genetic backgrounds of *B. subtilis*. Transcriptional *lacZ* fusions of WT promoters (P_{bceA} and P_{psdA}) as well as different sets of chimeras (BP1-4 and PB1-4) were integrated at the *amyE* locus of *B. subtilis* wildtype (WT), Δ*psdRS* strain (TMB1462) and Δ*bceRS* strain (TMB1460). Promoter activities were measured by β-galactosidase assay as described in Fig. 2. (C) BP1-4 in WT, (D) BP1-4 in Δ*psdRS* strain, (E) BP1-4 Δ*bceRS* strain, (F) PB1-4 in WT, (G) PB1-4 in Δ*bceRS* strain and (H) PB1-4 in Δ*psdRS* strain. Black and grey bars, induction with bacitracin and nisin, respectively; white bars, non-induced controls.

Figure S2. Unravelling the roles of different promoter elements in RR-promoter specificity. (A and B) Schematic of chimeric promoters derived from P_{bceA} and P_{psdA}, respectively. Composition of each chimeric promoter is indicated as follows: M, main binding site; L, linker; S, secondary binding site. MBS and SBS from P_{bceA} and P_{psdA} are indicated as in Fig.1. (C to H) Activities of chimeric promoters compared with WT promoters in different genetic backgrounds of *B. subtilis*. Transcriptional *lacZ* fusions of WT promoters (P_{bceA} and P_{psdA}) as well as different sets of chimeras from (A) and (B) were integrated at *amyE* locus in *B. subtilis* WT strain, Δ*psdRS* strain (TMB1462) and Δ*bceRS* strain (TMB1460). Promoter activities were measured by β-galactosidase assay as described for Fig. 2. (C) P_{bceA}-derived chimeras in WT, (D) P_{bceA}-derived chimeras in Δ*psdRS* strain, (E) P_{bceA}-derived chimeras in Δ*bceRS* strain, (F) P_{psdA}-derived chimeras in WT, (G) P_{psdA}-derived chimeras in Δ*bceRS* strain and (H) P_{psdA}-derived chimeras in Δ*psdRS* strain. Black bars and grey bars represent samples induced with bacitracin and nisin, respectively, while white bars stand for non-induced controls.

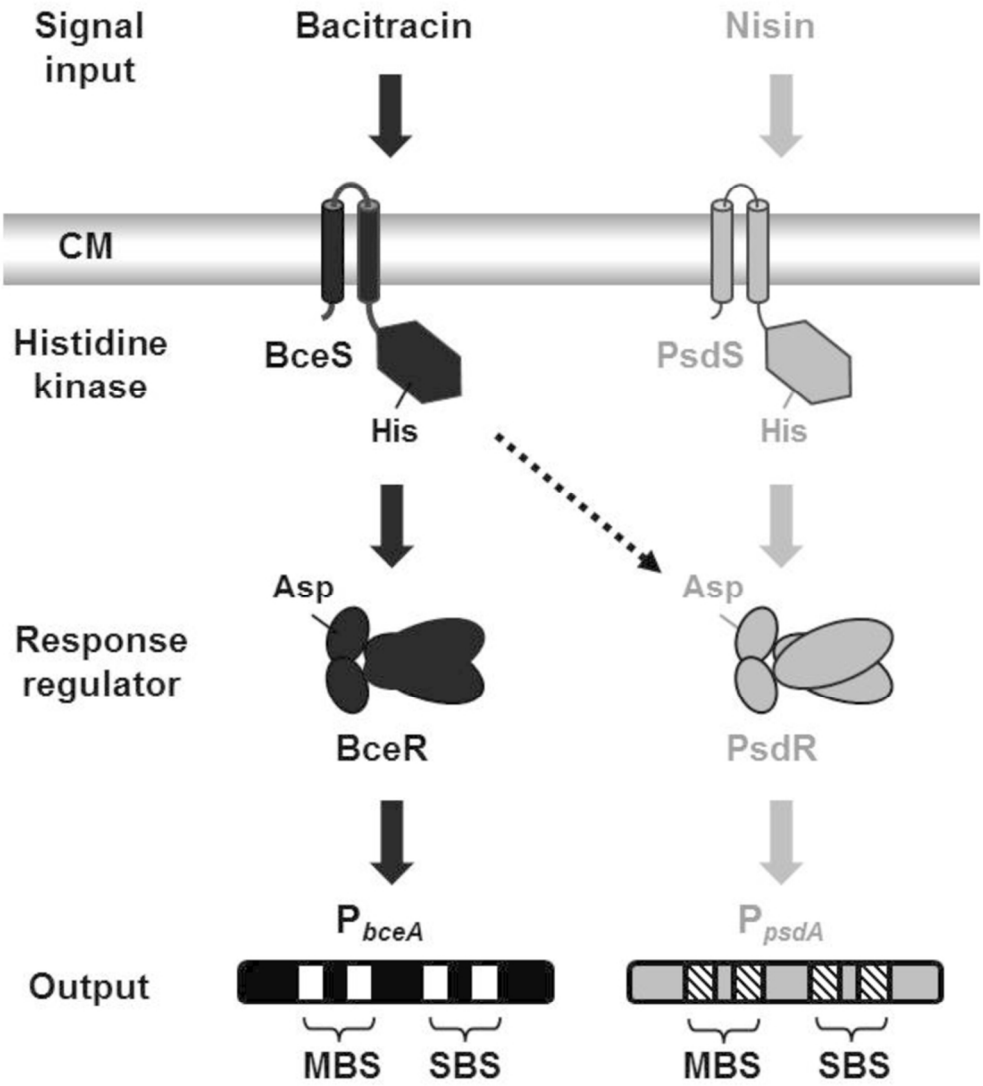

Figure 1. Model of signal transduction pathways of two Bce-like systems after induction with corresponding AMPs in Bacillus subtilis. The TCSs Bce and Psd and their inducing antibiotics as signal inputs are highlighted black and grey, respectively. For reasons of simplicity, the ABC transporters of both systems are not shown. Solid arrows indicate the signal transduction pathway within one system, while cross-regulation between BceS and PsdR is highlighted by the dotted arrow. On each promoter, MBS representing for the main binding site and SBS representing for the secondary binding of Bce-like RRs are filled with white on bceA promoter and slashes on psdA promoter. CM, cell membrane.

85x94mm (300 x 300 DPI)

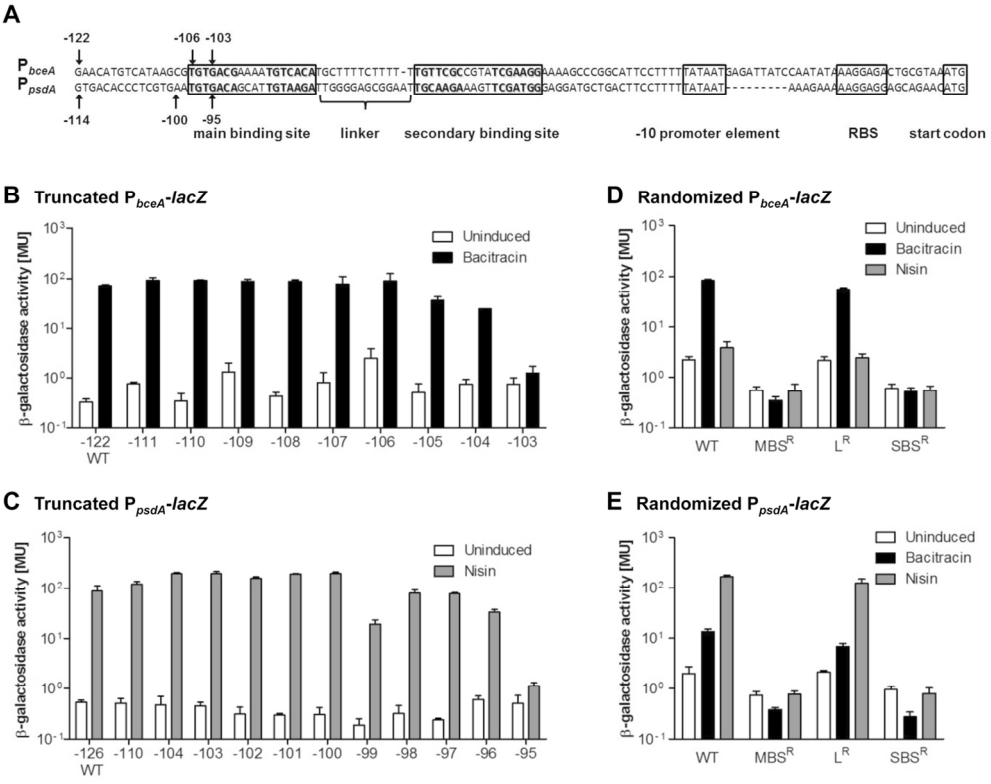

Figure 2. Functional analysis of bceA and psdA promoters of B. subtilis. (A) DNA sequence alignment of the bceA promoter and the psdA promoter. Different motifs are framed and annotated underneath the DNA sequence. Important positions on each promoter are marked with arrows according to the start codon of the corresponding regulated gene. Half binding sites of Bce-like RRs on each promoter are emphasized in bold face. Activities of (B) truncated constructions of the bceA promoter (from -122: +82 to -103: +82) and (C) truncated constructions of the psdA promoter (from -126: +30 to -95: +30) according to the start codon of regulated genes. Activities of (D) PbceA mutants and (E) PpsdA mutants with MBSR (main binding site random mutation), LR (linker random mutation) and SBSR (secondary binding site random mutation) are compared with the corresponding WT promoters. All promoter constructions were fused to lacZ and introduced into amyE locus of B. subtilis 168. Cultures growing exponentially in LB were challenged with Zn2+-bacitracin 30 μg ml-1 (black bars) or nisin 2 μg ml-1 (grey bars) for 30 min, comparing with the non-induced condition (white bars). β-galactosidase activities are expressed in Miller Units (MU) (Miller, 1972) and results are shown as the mean plus standard deviation of three biological replicates. A log scale is applied for reasons of clarity.

124x98mm (300 x 300 DPI)

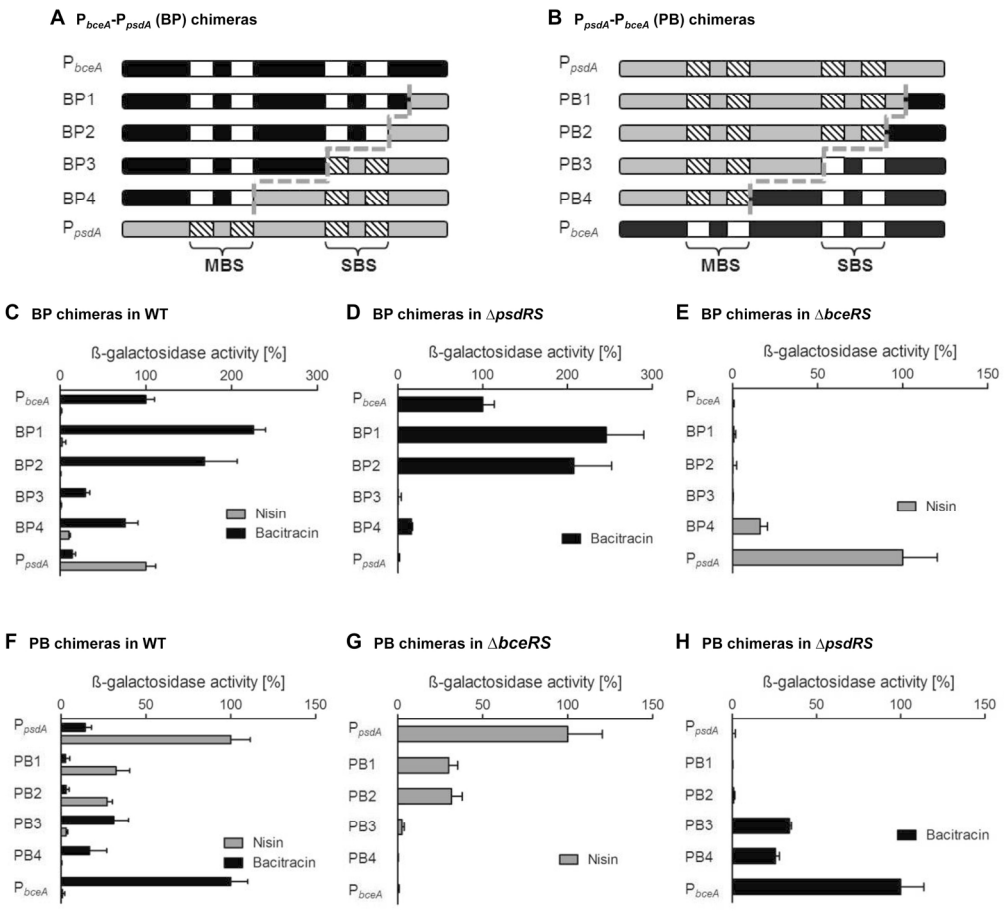

Figure 3. Functional studies of chimeric promoters derived from PbceA ("B") and PpsdA ("P"). Schematic of series of chimeric promoters (A) BP1-4, bceA promoter fragments (black) with gradual substitutions of 3' region by increased corresponding parts of psdA promoter (grey) and (B) PB1-4 vice versa are compared with WT PbceA and PpsdA. The MBS and SBS of PbceA and PpsdA are represented as in Fig.1. Grey dashed lines indicate the fusion points of each chimera. (C to H) Activities of chimeric promoters compared with WT promoters in different genetic backgrounds of B. subtilis. Transcriptional lacZ fusions of WT promoters (PbceA and PpsdA) as well as different sets of chimeras (BP1-4 and PB1-4) were integrated at the amyE locus of B. subtilis wildtype (WT), ΔpsdRS strain (TMB1462) and ΔbceRS strain (TMB1460). Promoter activities were measured by β-galactosidase assay as described in Fig. 2. (C) BP1-4 in WT, (D) BP1-4 in ΔpsdRS strain, (E) BP1-4 ΔbceRS strain, (F) PB1-4 in WT, (G) PB1-4 in ΔbceRS strain and (H) PB1-4 in ΔpsdRS strain. For reasons of clarity, the values of promoter activities induced by bacitracin are represented as % relative to the native PbceA, while the values of promoter activities induced by nisin are represented as % relative to the native PpsdA promoters. Both wild type promoters are set to 100% after subtraction of the uninduced promoter activities. The original data sets corresponding to Fig. 3 are provided in Fig. S1. Black and grey bars, induction with bacitracin and nisin, respectively.

173x161mm (300 x 300 DPI)

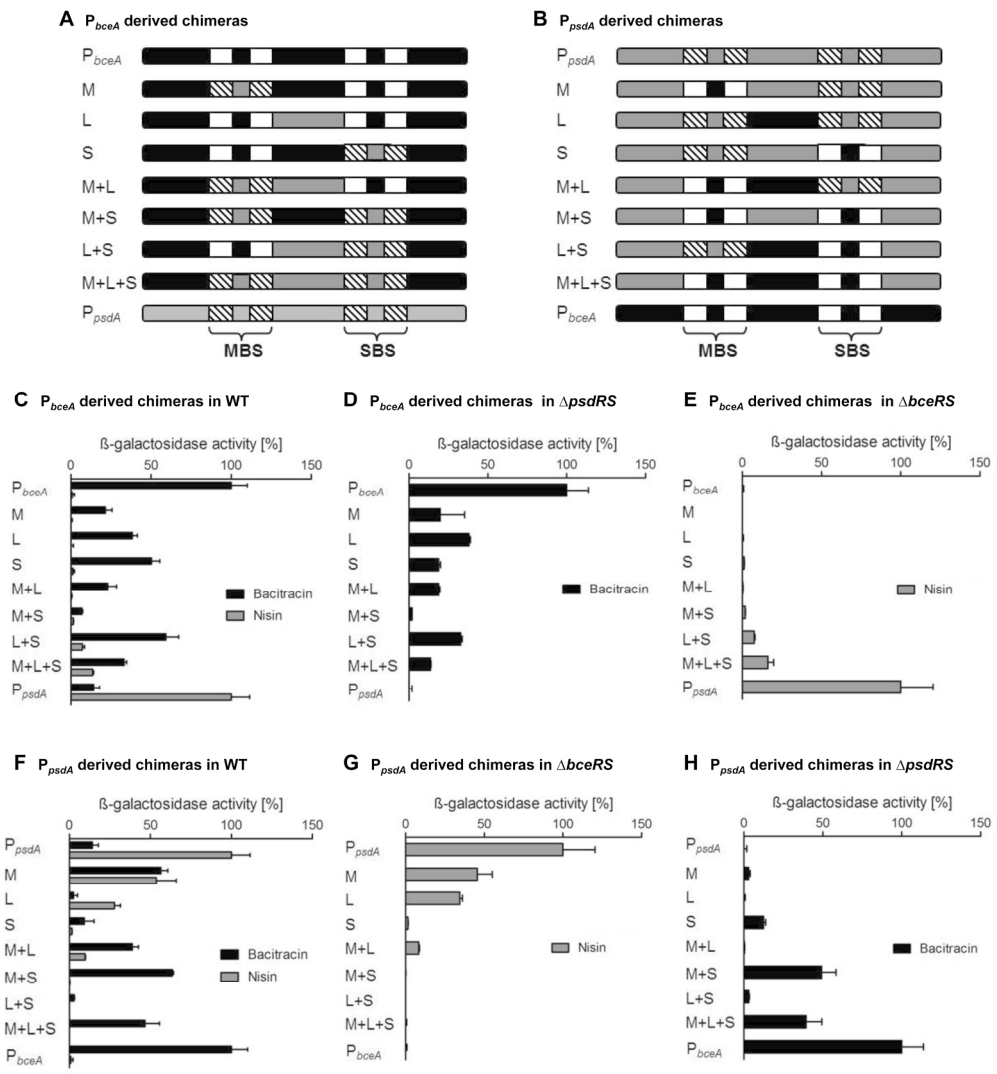

Figure 4. Unravelling the roles of different promoter elements in RR-promoter specificity. (A and B) Schematic of chimeric promoters derived from PbceA and PpsdA, respectively. Composition of each chimeric promoter is indicated as follows: M, main binding site; L, linker; S, secondary binding site. MBS and SBS from PbceA and PpsdA are indicated as in Fig.1. (C to H) Activities of chimeric promoters compared with WT promoters in different genetic backgrounds of B. subtilis. Transcriptional lacZ fusions of WT promoters (PbceA and PpsdA) as well as different sets of chimeras from (A) and (B) were integrated at amyE locus in B. subtilis WT strain, ΔpsdRS strain (TMB1462) and ΔbceRS strain (TMB1460). Promoter activities were measured by β-galactosidase assay as described for Fig. 2. (C) PbceA-derived chimeras in WT, (D) PbceA-derived chimeras in ΔpsdRS strain, (E) PbceA-derived chimeras in ΔbceRS strain, (F) PpsdA-derived chimeras in WT, (G) PpsdA-derived chimeras in ΔbceRS strain and (H) PpsdA-derived chimeras in ΔpsdRS strain. Black bars and grey bars represent samples induced with bacitracin and nisin, respectively. Data representation as described for Fig. 3; original data sets are provided in Fig. S2.

200x215mm (300 x 300 DPI)

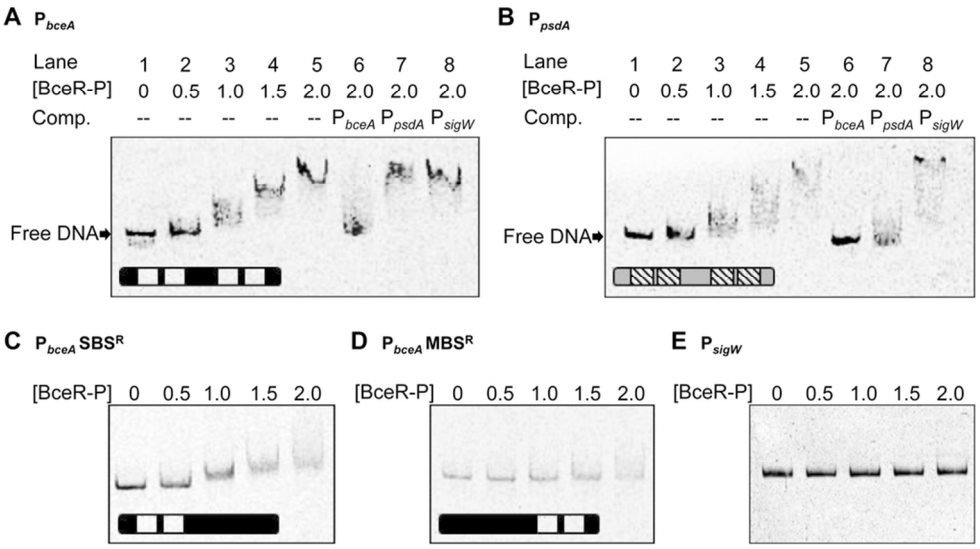

Figure 5. In vitro binding of BceR-P to PbceA and PpsdA. Increasing concentrations of phosphorylated 10×His-BceR were incubated with 30 fmol of different 6FAM-labeled promoter DNA fragments as follows: (A) PbceA from -122 to +82, (B) PpsdA from -126 to +30, (C) PbceA SBSR (SBS inactivated), (D) PbceA MBSR (MBS inactivated), and (E) PsigW as a negative control. Schematics of bceA-like promoters and corresponding mutants are shown in the lower left corner of each gel. The concentrations of phosphorylated BceR are indicated above the gel by [BceR-P] in μM. 900 fmol of unlabelled competitor (comp.) DNA fragments containing PbceA, PpsdA and PsigW were added for lanes 6, 7 and 8, respectively, in (A) and (B).

88x49mm (300 x 300 DPI)

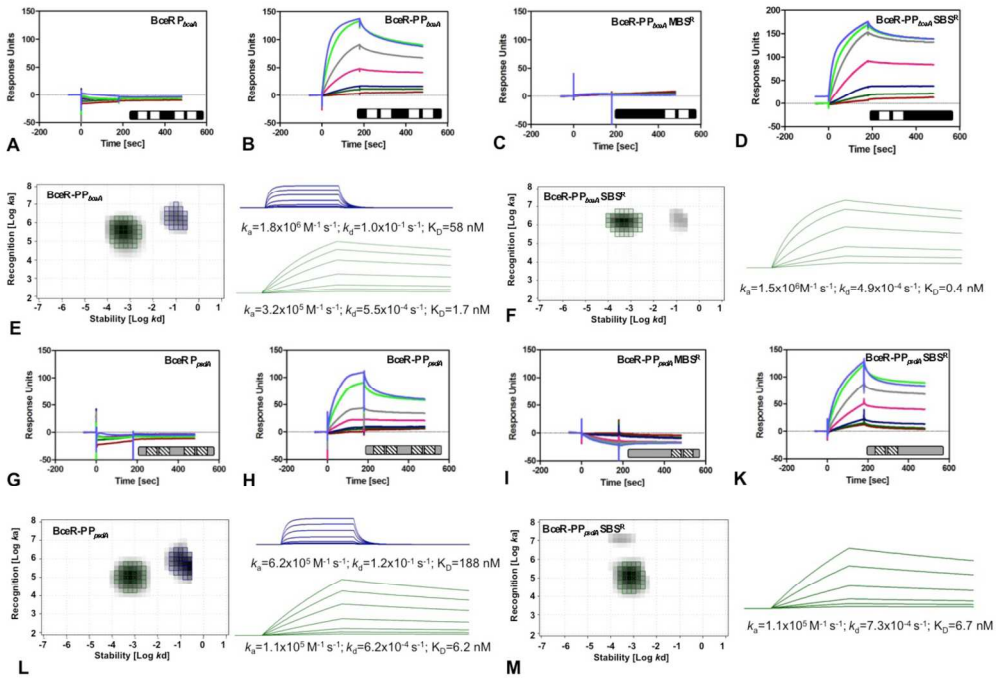

Figure 6. Surface plasmon resonance spectroscopy of and IM analysis BceR-P binding within the PbceA and PpsdA promoter region. (A) BceR binding to PbceA, (B) BceR-P binding to PbceA, (C) BceR-P binding to PbceA MBSR (MBS inactivated), and (D) BceR-P binding to PbceA SBSR (SBS inactivated), (E) IM and in silico sensorgrams of BceR binding to PbceA,; (F) IM and in silico sensorgrams of BceR binding to PbceA SBSR (SBS inactivated), (G) BceR binding to PpsdA, (H) BceR-P binding to PpsdA, (I) BceR-P binding to PpsdA MBSR, (K) BceR-P binding to PpsdA SBSR), (L) IM and in silico sensorgrams of BceR binding to PpsdA, and (M) IM and in silico sensorgrams of BceR binding to PpsdA SBSR (SBS inactivated). SPR sensorgrams: 0.2 nM (red line), 0.5 nM (brown line), 1 nM (dark blue line), 2.5 nM (magenta line), 5 nM (green line), 7.5 nM (lime green line), and 10 nM (blue line), respectively, of each of purified BceR or BceR-P was passed over the chip. The sensorgrams show each one representative example of three independently performed experiments. IM analyses: the blue spots in the IMs represent the fast ON/fast OFF interaction, which corresponds to the SBS, the green spots the slow ON/slow OFF interaction corresponding to the higher affine MBS. The respective calculated sensorgrams are shown in the same colors. The calculated overall affinities (KD), as well as the ON (ka) and OFF (kd) rates, are indicated below the respective in silico sensorgram. The grey shapes of the IM peaks represent the weighing factors meaning the darker the grey scale, the stronger the contribution.

170x117mm (300 x 300 DPI)

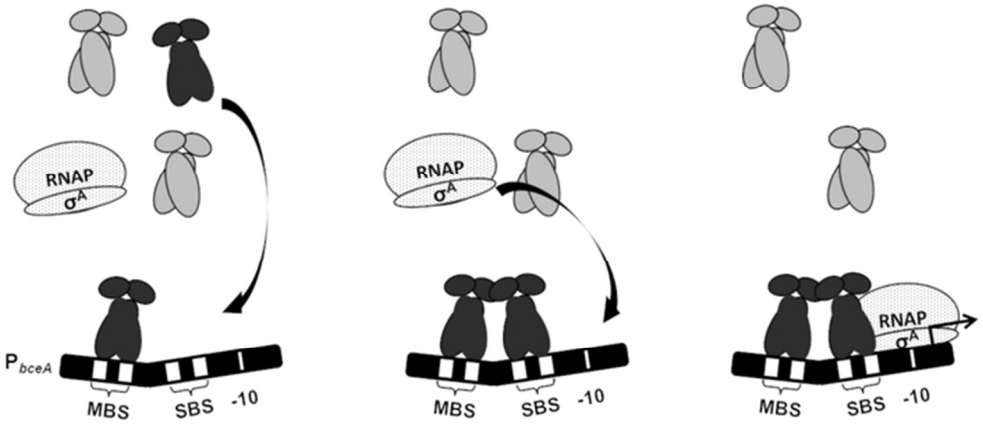

Figure 7. Model of the specific transcriptional activation of PbceA by BceR and RNA polymerase. Initially, a BceR dimer (black), but not a PsdR dimer (grey) preferentially binds to the MBS of PbceA. This interaction then facilitates the binding of a second BceR dimer to the SBS directly upstream of the -10 element of PbceA. This second binding event then mediates the binding of the σA subunit of the RNA polymerase holo-enzyme to the promoter region to ultimately initiate transcription. Presumably, the structure of the DNA is altered by the linker region between two binding sites (DNA bending). See discussion for details.

60x26mm (300 x 300 DPI)